

The Complex Spherical 2+4 Spin Glass: a Model for Nonlinear Optics in Random Media

F. Antenucci^{1,2}, A. Crisanti^{1,3} and L. Leuzzi^{2,1*}

¹ *Dipartimento di Fisica, Università di Roma “Sapienza”, Piazzale A. Moro 2, I-00185, Roma, Italy*

² *IPCF-CNR, UOS Kerberos Roma, Piazzale A. Moro 2, I-00185, Roma, Italy*

³ *ISC-CNR, UOS Sapienza, Piazzale A. Moro 2, I-00185, Roma, Italy*

A disordered mean field model for multimode laser in open and irregular cavities is proposed and discussed within the replica analysis. The model includes the dynamics of the mode intensity and accounts also for the possible presence of a linear coupling between the modes, due, e.g., to the leakages from an open cavity. The complete phase diagram, in terms of disorder strength, source pumping and non-linearity, consists of four different optical regimes: incoherent fluorescence, standard mode locking, random lasing and the novel spontaneous phase locking. A replica symmetry breaking phase transition is predicted at the random lasing threshold. For a high enough strength of non-linearity, a whole region with nonvanishing complexity anticipates the transition, and the light modes in the disordered medium display typical discontinuous glassy behavior, i. e., the photonic glass has a multitude of metastable states that corresponds to different mode-locking processes in random lasers. The lasing regime is still present for very open cavities, though the transition becomes continuous at the lasing threshold.

PACS numbers: 42.55.Zz, 42.60.Fc, 64.70.P-, 75.50.Lk

Considering salient multimode laser theory properties, both in ordered and disordered amplifying media, in this paper we construct a general statistical mechanical model for interacting waves. We study the model, in particular, in the framework of nonlinear optics, focusing on applications to the random lasing phenomenon. The term “random lasing” embraces a number of phenomena related to light amplification by stimulated emission in systems characterized by a spatial distribution of the electromagnetic field which is much more irregular and complicated than for well-defined cavity modes of standard lasing structures. In any system, to produce a laser two ingredients are essential: *optical amplification* and *feedback*. Amplified spontaneous emission can occur even without an optical cavity, and then the spectrum is determined only by the gain curve of the active material. Historically, already in the late 60’s Letokhov¹ theoretically discussed how light diffusion with gain can lead to the divergence of the intensity above a critical volume, and, if the gain depends on the wavelength, the emission spectrum narrows down close to the wavelength of maximum gain. These features were later observed in experiments.^{2,3} When the multiple-scattering feedback dominates, instead, lasing occurs: a phenomenon known as *Random Laser* (RL).⁴ The presence of feedback is associated with the existence of well-defined long-lived cavity modes and characterized by a definite spatial pattern of the electromagnetic field. A RL is, in other words, “*mirror-less*” but not “*mode-less*”⁵.

Among the most singular aspects of RLs is that, for systems composed by a large number of modes, a complex behavior in its temporal and spectral response is observed: if there is no specific frequency that dominates the others, the spectral resonances can change frequency from one excitation pulse to another, with emission spectra strongly fluctuating from shot to shot^{6–8} and

whose *shot-to-shot* correlations appear to be highly non-trivial⁹. In these systems the scattering particle positions and all external conditions are kept perfectly constant, so that these differences can only be due to the spontaneous emission occurring when the RL is activated at each pumping shot. In these conditions it is observed that the intensity distribution is not Gaussian, but rather of Levy type.^{10,11} This is true close to the lasing threshold (where the mentioned spectrum of fluctuations are expected⁵), whereas far below and far above the threshold the statistics remains Gaussian.

In the following we provide a general framework for the study of physical systems described by complex amplitudes coupled by both linear and nonlinear ordered or quenched disordered interaction terms. We follow a statistical mechanical approach to derive general results about the presence of a coherent regime and the type of transitions involved. Although the theory has a wide range of applications in modern physics, e. g., to the Bose - Einstein condensation¹², we focus on non-linear optics and the random lasing phenomenon.

The use of statistical mechanics of disordered systems for random lasers was initially introduced in Ref. [13] for a phase model where, using the *replica method*,¹⁴ was found that the competition for the available gain of a large number of random modes can lead to a behavior similar to that of a discontinuous glass transition.^{15–18} Successive applications of the replica method to this problem^{19–21} have shown that non-linear optics and random lasers can be a benchmark for the modern theory of glassy systems.

In the present study we consider a more general and realistic model for non-linear waves by removing the two basic assumptions of earlier works: the quenched amplitude approximation and the strong cavity limit. We will consider the whole complex amplitudes of the elec-

tromagnetic field eigenmodes expansion, not only the phases, as the dynamic variables of the problem and we will account for the presence of nonzero off-diagonal elements in the linear coupling, as expected in presence of an irregular and/or open resonator. The inclusion of the intensity dynamics, in particular, could open new and more practical ways to directly compare with experiments, cf., e.g., Ref. [9 and 22], since the mode intensities are usually more easily accessible than the phases. Some results of this study have been presented in Ref. [23].

The statistical mechanics of disordered systems provides a peculiar point of view on this RL phenomenon: the leading mechanism for the non-deterministic activation of the modes in this complex coherent wave regime is identified in the frustration of the disordered interactions and the consequent presence of many degenerate equivalent glassy states.^{20,21}

The paper is organized as follows: in Sect. I we present and discuss the multimode laser theory for open resonators in the semiclassical limit^{24,25} that will be the starting point for our statistical mechanical model. In Sect. II we discuss the disordered mean field model and define the control parameters. In Sect. III we report the results of the replica analysis of the disordered model and discuss the type of phases and transitions predicted. In particular, in Sect. III C we examine the presence of a region in the phase diagram with a nonzero complexity. Finally in Sect. IV we draw our conclusions.

I. MULTIMODE LASER THEORY

The complex structure and the extreme openness of Random Lasers make these optical systems different from traditional cavity lasers. From a theoretical point of view, the strong coupling to the external world requires a different treatment from the standard approach of traditional laser textbooks.

The problem of describing quantum systems strongly interacting with the environment has large interest and it is relevant not only for the physics of lasers (see, e. g., Ref [26]). The difficulty originates from the non-Hermiticity of the problem as the openness becomes relevant, so that the standard methods to solve or quantize Hermitian operators do not apply in this case. The quantum system is localized in space. However, there is always a natural environment into which the quantum system with discrete states is embedded. The environment consists of the continuum of extended scattering states into which the discrete states of the system are embedded and can decay. The coupling matrix between the discrete states of the system and the scattering states of the continuum determine the lifetime of the states, which is, therefore, usually finite.

Several approaches are presented in literature to build a set of modes suitable for a separation of time and coordinates dependencies of various physical observables, in particular the electric and magnetic fields.^{27–30} Here, we

start from the system-and-bath approach of Ref. [31], in which a rigorous quantization of the field is possible. We note, in particular, that the quantum treatment is necessary to compute the linewidth or the photon statistics of the output radiation. In this approach, the contributions of radiative and localized modes can be separated by the Feshbach projection method onto two orthogonal subspaces.³² This leads to an effective theory in the subspace of localized modes with an effective linear off-diagonal damping coupling.^{31,33,34}

The atom-field system can, then, be described via the complex amplitudes of the localized electromagnetic modes α_λ and the atomic raising operator $\sigma_-^\dagger = |e\rangle\langle g|$ and inversion operator $\sigma_z = |e\rangle\langle e| - |g\rangle\langle g|$, being $|g\rangle$ and $|e\rangle$ the ground and excited atom states. The evolution of the operators can be expressed by the Jaynes-Cumming Hamiltonian,^{35,36} and, including the cavity loss, is expressed in the Heisenberg representation as²⁴

$$\dot{\alpha}_\lambda = -i\omega_\lambda \alpha_\lambda - \sum_\mu \gamma_{\lambda\mu} \alpha_\mu \quad (1)$$

$$+ \int d\mathbf{r} g_\lambda^\dagger(\mathbf{r}) \sigma_-(\mathbf{r}) + F_\lambda, \quad (2)$$

$$\dot{\sigma}_-(\mathbf{r}) = -(\gamma_\perp + i\omega_a) \sigma_-(\mathbf{r}) + 2 \sum_\mu g_\mu(\mathbf{r}) \sigma_z(\mathbf{r}) \alpha_\mu + F_-(\mathbf{r}), \quad (3)$$

$$\dot{\sigma}_z(\mathbf{r}) = \gamma_\parallel (S\rho(\mathbf{r}) - \sigma_z(\mathbf{r})) - \sum_\mu (g_\mu^\dagger(\mathbf{r}) \alpha_\mu^\dagger \sigma_-(\mathbf{r}) + \text{h.c.}) + F_z(\mathbf{r}),$$

where $\gamma_{\lambda\mu}$ is the damping matrix associated to the openness of the cavity,^{31,33} $\rho(\mathbf{r})$ the atom density, ω_a the frequency of the atomic transition, γ_\perp the polarization decay rate, γ_\parallel the population-inversion decay rate and S the pump intensity resulting from the interaction between the atoms and the external bath. The noise term F_λ follows from the coupling with the bath. The field-atoms coupling constants are

$$g_\lambda(\mathbf{r}) \equiv \frac{\omega_a p}{\sqrt{2\hbar\epsilon_0\omega_\lambda}} \mu_\lambda(\mathbf{r}), \quad (4)$$

where p is the atomic dipole matrix element and the $\mu_\lambda(\mathbf{r})$ are the orthogonal set of the resonator eigenstates.^{31,33} The interaction also gives rise to the noises $F_-(\mathbf{r})$ and $F_z(\mathbf{r})$, due, for example, to the finite lifetime of the excited states for the decay to states not involved in the stimulated emission process.

The semiclassical theory consists in replacing the operators with their expectation values. It is assumed that the lifetimes of the modes are much longer than the characteristic times of pump and loss: the atomic variables can then be adiabatically removed to obtain the (non-linear) equations for the field alone.

Consider first the case of weak pumping, so that it is possible to assume $\sigma_z(\mathbf{r}) = S\rho(\mathbf{r})$ and the unique stationary solution is $\alpha_\lambda = 0$ for all the modes. In this case the deviations from the stationary state relax to zero with

complex frequency ω_k given by the eigenvalues of the non-Hermitian matrix²⁴

$$H_{\lambda\mu} = \omega_\lambda \delta_{\lambda\mu} - i\gamma_{\lambda\mu} + iG_{\lambda\mu}^{(2)}(\omega_k), \quad (5)$$

with $G_{\lambda\mu}^{(2)}(\omega) \equiv 2S \int d\mathbf{r} \rho(\mathbf{r}) \frac{g_\mu^*(\mathbf{r})g_\lambda(\mathbf{r})}{i(\omega_a - \omega) + \gamma_\perp}$.

In general, if the cavity is open and/or the atoms are not uniformly distributed in the resonator, the matrix $H_{\lambda\mu}$ is not diagonal: the eigenvalues and eigenvectors are, hence, different from the case of cold cavity and depend parametrically on the pump strength S . In particular, increasing S the eigenvalues move up in the complex plane. The lasing threshold is reached when one eigenvalue takes a positive imaginary part. In this case the gain exceeds the loss and the solution $\alpha_\lambda = 0$ becomes unstable.

At the lasing threshold is, then, necessary to consider the time evolution of the atom operators that provides an effective non-linear coupling among the electromagnetic modes. In this case the standard approach is to consider an expansion in power of the mode amplitudes. One starts neglecting the quadratic term in Eq. (3) obtaining the zero-order approximation, that replaced in Eq. (2) gives the first order approximation that replaced back in Eq. (3) gives the second-order approximation and so forth. Inserting the result into Eq. (1) one can construct a perturbative approximation of the effective evolution of the mode amplitudes.

In the particular case of the *free-running approximation*,²⁴ that is assuming that the different lasing modes oscillate independently from each other (so that the phases are uncorrelated and the interaction concerns the intensities alone), it is possible to resum the equation and obtain an expression for the mode intensities valid to all the orders in the perturbation theory (cf. Ref. [25]). This approximation may be valid for the so-called non-resonant or incoherent feedback emission in disordered cavities,¹ where the interference effects do not play any role. In this case the emission is due solely to amplified spontaneous emission, and, then, the spectrum is determined only by the gain curve of the active material. This approach explains some simple properties of emission from disordered cavities.^{2,3} For the lasing regime, however, it is the multiple-scattering induced feedback that defines optical modes, with a well resolved frequency, a given bandwidth and spatial profile.⁵ It, thus, becomes essential to include the phases into the analysis and consider the non-linear interactions non-perturbatively.

Since we are mainly interested in the characterization of the random lasing regime, we do not assume the free-running approximation and limit ourselves to the non-linear third order theory. The subsequent orders may become relevant far above the threshold. From a statistical mechanics point of view the orders beyond the third are not expected to change the universality class of the transition for a large class of models (see, e. g., Ref. [37]).

Being specific, if one considers $g^2|a|^2 \ll \gamma_\perp \gamma_\parallel$, where $|a|^2$ is the typical intensity in the lasing regime, the third order theory is exact.

A. Cold Cavity vs Slow Amplitude Modes

The evolution in the lasing regime is conveniently expressed in the basis of the slow amplitude modes. A *slow amplitude mode* with index l is a solution such that it has a harmonic form for $t \gg 1$ and, therefore, its Fourier transform is proportional to $\delta(\omega - \omega_l)$. By definition, a *lasing mode* is a slow amplitude mode with a positive intensity at the solution. In general the lasing modes are different from the cold cavity ones. The steady-state solutions are different already in the linear regime, as $G_{\lambda\mu}^{(2)}$ is not diagonal, cf. Eq. (5). We express the relationship between cold cavity modes α_λ and laser modes a_k in the form

$$\alpha_\lambda(t) = \sum_k A_{\lambda k} \bar{a}_k(t), \quad \bar{a}_k(t) = a_k(t) e^{-i\omega_k t} \quad (6)$$

with $a_k(t)$ evolving on time scales much longer than ω_k^{-1} , so that $\bar{a}_k(\omega) \simeq \delta(\omega - \omega_k)$. Here and in the following we use Greek letters for cold cavity modes and Latin letters for the slow amplitude modes.

We consider a complete *slow amplitude modes basis* in order to expand any mode and, in particular, invert Eq. (6)

$$\bar{a}_k(t) = \sum_\lambda B_{k\lambda}^* \alpha_\lambda(t) \quad , \quad B_{k\lambda}^* = (A_{k\lambda})^{-1} . \quad (7)$$

Using the expansion in the slow amplitude modes we can express the mode evolution Eq. (1) at the third order as

$$\dot{a}_l(t) = \sum_{k|FMC(l,k)} \left[\tilde{\gamma}_{lk} - S G_{lk}^{(2)} \right] a_k(t) - S \sum_{\mathbf{k}|FMC(l,\mathbf{k})} G_{l\mathbf{k}}^{(4)} a_{k_1}(t) a_{k_2}^*(t) a_{k_3}(t), \quad (8)$$

where the sums are restricted to terms that meet the *frequency matching conditions* (FMC) (see below), the matrix $\tilde{\gamma}_{lk}$ is

$$\tilde{\gamma}_{lk} \equiv \sum_{\lambda\mu} B_{\lambda l}^* \gamma_{\lambda\mu} A_{\mu k}, \quad (9)$$

with the left and right coupling constants for the slow amplitude modes given by

$$g_k^L = \sum_\mu B_{\mu k} g_\mu, \quad g_k^R = \sum_\mu A_{\mu k} g_\mu, \quad (10)$$

and $G_{lk}^{(2)}$ and $G_{l\mathbf{k}}^{(4)}$ are functions of the frequencies ω_k :

$$G_{lk}^{(2)} = M_k^{(2)} \int d\mathbf{r} \rho(\mathbf{r}) g_l^{L*}(\mathbf{r}) g_k^R(\mathbf{r}), \quad (11)$$

$$G_{l\mathbf{k}}^{(4)} = M_{\mathbf{k}}^{(4)} \int d\mathbf{r} \rho(\mathbf{r}) g_l^{L*}(\mathbf{r}) g_{k_1}^R(\mathbf{r}) g_{k_2}^{R*}(\mathbf{r}) g_{k_3}^R(\mathbf{r}). \quad (12)$$

The coefficients $M_k^{(2)}$ and $M_{\mathbf{k}}^{(4)}$ are defined as

$$\begin{aligned} M_k^{(2)} &\equiv -\frac{1}{\pi\gamma_{\perp}} D(\omega_k), \\ M_{\mathbf{k}}^{(4)} &\equiv \frac{D(\omega_{k_3}) + D^*(\omega_{k_2})}{2\pi^3\gamma_{\perp}^2\gamma_{\parallel}} \\ &\quad \times D(\omega_{k_1} - \omega_{k_2} + \omega_{k_3}) D_{\parallel}(\omega_{k_3} - \omega_{k_2}) \end{aligned} \quad (13)$$

with

$$D_{\parallel}(\delta\omega) \equiv \left(1 - i\frac{\delta\omega}{\gamma_{\parallel}}\right)^{-1}, \quad D(\omega) \equiv \left(1 - i\frac{\omega - \omega_a}{\gamma_{\perp}}\right)^{-1} \quad (14)$$

The notation $\sum_{\mathbf{k}|\text{FMC}(l,\mathbf{k})}$ introduced in Eq. (8) denotes that the slow amplitude condition $\bar{a}_k(\omega) \simeq \delta(\omega - \omega_k)$ restricts the sums to modes (l, \mathbf{k}) that meet the frequency matching condition. For generic $k_1 \dots, k_{2n}$ interacting modes the FMC reads:

$$\text{FMC}(\mathbf{k}) : |\omega_{k_1} - \omega_{k_2} + \dots + \omega_{k_{2n-1}} - \omega_{k_{2n}}| \lesssim \gamma. \quad (15)$$

The finite linewidth γ of the modes can be thoroughly derived only in a complete quantum theory. In particular, the noise factors in Eqs. (1)-(3) have to be included, resulting in a weak time dependence of $\bar{a}_k(t)$ in Eq. (6). Here, we include it in an effective way, as a parameter to suitably conform to different experimental situations.

We stress as, in general, the linear term of Eq. (8) may have non-zero off-diagonal terms. They are all zero when the frequencies are well distinct, i.e., the spectral interspacing $\delta\omega \gg \gamma$, so that the frequency matching condition of the linear term is never satisfied but for the modes with overlapping frequency. While this is generally true for standard high quality-factor lasers,³⁸ for RL there can be a significant frequency overlap between the lasing modes, $\delta\omega \sim \gamma$, and off-diagonal linear contributions must be considered in the slow amplitude basis.

The actual values of the couplings are in principle, and in some simple case, entirely computable in the cold cavity basis, cf. Eqs. (11)-(12) and, e. g., Ref. [34]. The main problem remains how to express the interactions in the slow amplitude mode basis actually used in the dynamics. In some cases the solution can be found using some self-consistent procedures proceeding iteratively starting from the solution obtained without the non-linear coupling.³⁹⁻⁴¹ In particular, when the non-linear term is entirely neglected, a possible (though not unique) solution is the one that diagonalizes the linear interaction. Nonetheless, when the lasing threshold is exceeded, the non-linear term becomes non-perturbatively relevant and the diagonalization of the linear term does not correspond to a slow amplitude basis in the most general case of lasing in random media.

B. The role of the noise

In the previous semiclassical derivation we have neglected all noise sources. However, to obtain a complete statistical description the noise, and, hence, the spontaneous emission and the heat-bath temperature, must be taken into account. Indeed, we will show that the role of the entropy becomes crucial for disordered multimode lasers, where a random first order transition⁴² is expected, at least in the mean-field approximation.

In general, different noise sources occur (see F_{λ} , F_{-} and F_z in Eqs. (1)-(3)). Further on, in the case of open cavities, it is known that the noise F_{λ} due to the external bath coupling is correlated in the cold cavity modes basis.^{31,33} We, then, consider the presence of a noise $F_l(t)$ in Eq. (8):

$$\begin{aligned} \langle F_{k_1}^*(t_1) F_{k_2}(t_2) \rangle &= 2T \Gamma_{k_1 k_2} \delta(t_1 - t_2), \\ \langle F_{k_1}(t_1) F_{k_2}(t_2) \rangle &= 0, \end{aligned} \quad (16)$$

with T being the spectral power of the noise, proportional to the heat-bath temperature. The matrix $\Gamma_{k_1 k_2}$ corresponds to the damping matrix Eq. (9) for F_{λ} and, in general, is non diagonal for open cavities. It can be, though, diagonalized, at the possible price of having a non-diagonal linear contribution in Eq. (8). Indeed, a non-unitary change of basis affects the noise correlation:

$$a_l = \sum_{\lambda} A_{l\lambda}^{-1} \alpha_{\lambda} \quad \rightarrow \quad F_l = \sum_{\lambda} A_{l\lambda}^{-1} F_{\lambda}$$

and

$$\langle F_{k_1}^*(t_1) F_{k_2}(t_2) \rangle = \sum_{\lambda_1 \lambda_2} (A^*)_{l_1 \lambda_1}^{-1} \langle F_{\lambda_1}^*(t_1) F_{\lambda_2}(t_2) \rangle A_{l_2 \lambda_2}^{-1}$$

The decomposition in the slow amplitude modes, Eq. (6), is by no means unique. This freedom may be used to build a mode basis where the noise is uncorrelated. In the following, we assume that the various independent noise sources act so that such basis construction is possible and, hence, the noise can be assumed white and uncorrelated also in the general case of open and irregular cavities. We will, consequently, consider Gaussian, white and uncorrelated noise:

$$\begin{aligned} \langle F_{k_1}^*(t_1) F_{k_2}(t_2) \rangle &= 2T \delta_{k_1 k_2} \delta(t_1 - t_2), \\ \langle F_{k_1}(t_1) F_{k_2}(t_2) \rangle &= 0, \end{aligned} \quad (17)$$

However, since diagonalization of the noise terms may result in possible off-diagonal terms in the linear coupling in Eq. (8), independent from the presence of the non-linear interaction, off-diagonal linear interaction is, thus, considered throughout the rest of the paper.

In analogy with the standard mode locking case,⁴³ we,

hence, eventually define the complex valued functional

$$\begin{aligned}
\mathcal{H} &= - \sum_{\mathbf{k}|\text{FMC}(\mathbf{k})} \left[\tilde{g}_{k_1 k_2} - S G_{k_1 k_2}^{(2)} \right] a_{k_1}^* a_{k_2} \\
&+ \sum_{\mathbf{k}|\text{FMC}(\mathbf{k})} S G_{k_1 k_2 k_3 k_4}^{(4)} a_{k_1} a_{k_2}^* a_{k_3} a_{k_4}^* \\
&\equiv \sum_{\mathbf{k}|\text{FMC}(\mathbf{k})} g_{k_1 k_2}^{(2)} a_{k_1} a_{k_2}^* \\
&+ \frac{1}{2} \sum_{\mathbf{k}|\text{FMC}(\mathbf{k})} g_{k_1 k_2 k_3 k_4}^{(4)} a_{k_1} a_{k_2}^* a_{k_3} a_{k_4}^* \quad (18)
\end{aligned}$$

where again the sums are restricted by the FMC (15), yielding the complex Langevin equation for the stochastic dynamics of the amplitudes

$$\dot{a}_k = - \frac{\partial \mathcal{H}}{\partial a_k^*} + F_l \quad (19)$$

Eq. (18) can be rewritten in terms of its real and imaginary parts $\mathcal{H}_R + i\mathcal{H}_I$:

$$\begin{aligned}
\mathcal{H}_R &= \sum_{\mathbf{k}|\text{FMC}(\mathbf{k})} G_{k_1 k_2} a_{k_1} a_{k_2}^* \\
&+ \frac{1}{2} \sum_{\mathbf{k}|\text{FMC}(\mathbf{k})} \Gamma_{k_1 k_2 k_3 k_4} a_{k_1} a_{k_2}^* a_{k_3} a_{k_4}^*, \\
\mathcal{H}_I &= \sum_{\mathbf{k}|\text{FMC}(\mathbf{k})} D_{k_1 k_2} a_{k_1} a_{k_2}^* \\
&+ \frac{1}{2} \sum_{\mathbf{k}|\text{FMC}(\mathbf{k})} \Delta_{k_1 k_2 k_3 k_4} a_{k_1} a_{k_2}^* a_{k_3} a_{k_4}^*,
\end{aligned}$$

with

$$G_{k_1 k_2} \equiv \frac{1}{2} \left(g_{k_1 k_2}^{(2)} + g_{k_2 k_1}^{(2)*} \right), \quad (20)$$

$$\Gamma_{k_1 k_2 k_3 k_4} \equiv \frac{1}{2} \left(g_{k_1 k_2 k_3 k_4}^{(4)} + g_{k_2 k_1 k_4 k_3}^{(4)*} \right) \quad (21)$$

$$iD_{k_1 k_2} \equiv \frac{1}{2} \left(g_{k_1 k_2}^{(2)} - g_{k_2 k_1}^{(2)*} \right), \quad (22)$$

$$i\Delta_{k_1 k_2 k_3 k_4} \equiv \frac{1}{2} \left(g_{k_1 k_2 k_3 k_4}^{(4)} - g_{k_2 k_1 k_4 k_3}^{(4)*} \right). \quad (23)$$

Considering, as well, real and imaginary parts of mode amplitudes $a_l \equiv \sigma_l + i\tau_l$, the stochastic Eq. (19) can be expressed as

$$\begin{aligned}
\frac{\partial \sigma_l}{\partial t} &= - \frac{1}{2} \frac{\partial \mathcal{H}_R}{\partial \sigma_l} + \frac{1}{2} \frac{\partial \mathcal{H}_I}{\partial \tau_l} + F_l^R, \\
\frac{\partial \tau_l}{\partial t} &= - \frac{1}{2} \frac{\partial \mathcal{H}_R}{\partial \tau_l} - \frac{1}{2} \frac{\partial \mathcal{H}_I}{\partial \sigma_l} + F_l^I. \quad (24)
\end{aligned}$$

From Eqs. (24) it is clear that \mathcal{H}_R is associated with a purely dissipative motion (a gradient flow in the $2N$ dimensional space $\sigma_1, \dots, \sigma_N, \tau_1, \dots, \tau_N$), while \mathcal{H}_I generates a purely Hamiltonian motion for the N conjugated variables (σ_l, τ_l) . If $\mathcal{H}_R = 0$ the total optical intensity

$\mathcal{E} \equiv \sum_k |a_k|^2$ is a constant of motion under the previous Langevin equations (like \mathcal{H} itself). When $\mathcal{H}_R \neq 0$ this is no longer true, though the system is still stable because the gain decreases as the optical intensity increases.⁴⁴ For standard lasers this is usually modeled assuming that the gain is such that

$$G_{kk} = \frac{G_0}{1 + \mathcal{E}/E_{\text{sat}}}, \quad \forall k \quad (25)$$

where E_{sat} is the saturation power of the amplifier. To study the equilibrium properties of the model, it is possible to consider a simpler model: at any instant the gain is supposed to assume exactly the value that keeps \mathcal{E} a constant of the motion, as Gordon and Fisher have proposed in Ref. [43]. In this way the system evolves over the hypersphere $\mathcal{E} \equiv \mathcal{E}_0$.

The relation between the thermodynamics in the fixed-power ensemble and a variable-power ensemble might be seen as similar to the relation between the canonical and grand canonical ensembles in statistical mechanics.⁴⁵ The constraint $\mathcal{E} \equiv \mathcal{E}_0$ will induce a correlation of order N^{-1} in the noise F_l . However, as far as we are interested in the limit $N \gg 1$, such correlation can be neglected and the noise considered as white.

The request $\partial \mathcal{E} / \partial t = 0$ implies that G_0 , expressed as $G_{kk} \equiv G_0 + G_{kk}^\delta$, is given by

$$\begin{aligned}
\mathcal{E} G_0 &= - \sum_{\mathbf{k}|\text{FMC}(\mathbf{k})} G_{k_1 k_2}^\delta a_{k_1} a_{k_2}^* \\
&- \sum_{\mathbf{k}|\text{FMC}(\mathbf{k})} \Gamma_{k_1 k_2 k_3 k_4} a_{k_1} a_{k_2}^* a_{k_3} a_{k_4}^*.
\end{aligned}$$

In particular for $G_{k_1 k_2}^\delta = G_{k_1}^\delta \delta_{k_1 k_2}$ and $\Gamma_{k_1 k_2 k_3 k_4} = \Gamma$, the known result for the standard mode-locking case is recovered.⁴³ Inserting this expression for G_0 in the Langevin equations (19), one finds that in this case the functional \mathcal{H}_R becomes

$$\begin{aligned}
\mathcal{H}_R &\equiv - \frac{\mathcal{E}_0}{\mathcal{E}} \sum_{\mathbf{k}|\text{FMC}(\mathbf{k})} G_{k_1 k_2}^\delta a_{k_1} a_{k_2}^* \\
&- \frac{\mathcal{E}_0^2}{2\mathcal{E}^2} \sum_{\mathbf{k}|\text{FMC}(\mathbf{k})} \Gamma_{k_1 k_2 k_3 k_4} a_{k_1} a_{k_2}^* a_{k_3} a_{k_4}^*. \quad (26)
\end{aligned}$$

where now coupling coefficients G^δ and Γ do not depend from complex amplitudes a 's. This expression for the Hamiltonian includes the condition that the total optical power \mathcal{E} is a constant of motion. Imposing the spherical constraint simplifies the coefficients $\mathcal{E}_0/\mathcal{E} = 1$.

C. Purely Dissipative Case

In the case $\mathcal{H}_R \gg \mathcal{H}_I$ the functional \mathcal{H} is approximately real. For the standard mode-locking lasers this corresponds to the physical situation where the group velocity dispersion and the Kerr effect can be neglected.³⁸

The purely dissipative case does also apply to the important case of soliton lasers.⁴⁶ In the general case of Eq. (18) the situation is more complex. If the coefficients $g_{k_1 k_2}^{(2)}$ and $g_{k_1 k_2 k_3 k_4}^{(4)}$ are real then the imaginary part of \mathcal{H} clearly vanishes, see Eqs. (22,23). The requirement of real coefficients is, however, not necessary to ensure a real valued \mathcal{H} , cf. Eq. (18), of the form given by Eq. (26). A less strict, though sufficient condition is that, cf. Eqs. (6), (14),

$$A_{\lambda l} = A_{l\lambda}^*; \quad \omega_l - \omega_a \ll \gamma_{\perp}; \quad \delta\omega \ll \gamma_{\parallel} \quad (27)$$

This is consistent with, but stronger than, the usual rotating-wave approximation, $\delta\omega \ll \omega_l, \forall l$.

The case with a real functional \mathcal{H} is of particular interest because it can be studied using the standard methods of the equilibrium statistical physics. In fact, when the functional \mathcal{H} is real, the Eqs. (24) reduce to the familiar “potential form”: the evolution is the derivative of a “potential” respect to the considered variables plus white Gaussian noise. Hence, the steady-state solution of the associated Fokker-Plank equation

$$\begin{aligned} \dot{\rho} = & - \sum_k \frac{\partial}{\partial \sigma_k} \left\{ \frac{\partial \mathcal{H}_R}{\partial \sigma_k} \rho \right\} - \sum_k \frac{\partial}{\partial \tau_k} \left\{ \frac{\partial \mathcal{H}_R}{\partial \tau_k} \rho \right\} \\ & + T \sum_k \left(\frac{\partial^2}{\partial \sigma_k^2} + \frac{\partial^2}{\partial \tau_k^2} \right) \rho \end{aligned} \quad (28)$$

is given by the familiar Gibbs distribution

$$\rho(\sigma_1, \tau_1 \dots \sigma_N, \tau_N) = \frac{e^{-\mathcal{H}_R/T_{\text{ph}}}}{\int e^{-\mathcal{H}_R/T_{\text{ph}}} d\sigma_1 d\tau_1 \dots d\sigma_N d\tau_N}. \quad (29)$$

where T_{ph} is an effective “photonic” temperature proportional to the heat-bath temperature. This case, then, is the most interesting for the application of statistical mechanics and it will be analyzed in this paper.

The general case of $\mathcal{H}_I \neq 0$ is harder to study analytically. We note that, in general, it is expected that transitions of the first order are not removed by slight modification of the dynamics. The analysis of the complete complex Langevin dynamics is postponed to a future work.

II. THE STATISTICAL MECHANICS APPROACH

In the rest of this work we shall discuss the properties of mean-field solution of the model described by the Hamiltonian Eq. (26) with the global *spherical*⁴⁷ constraint $\mathcal{E} \equiv \sum_k |a_k|^2 = \mathcal{E}_0$. We notice that, because of this constraint on the power, adding a constant diagonal term to the pairwise coupling is irrelevant for the thermodynamics of the system.

The mean-field solution is exact when the probability distribution of the couplings is the same for all the mode

couples (k_1, k_2) and quadruplets (k_1, k_2, k_3, k_4) . This corresponds to the physical situation in which the two following conditions hold:

- *narrow-bandwidth*: the linewidth of the mode frequencies γ is comparable with the total emission bandwidth $\Delta\omega$ so that the frequency-matching conditions are always satisfied, cf. Eq. (15);
- *extended modes*: all the mode localizations are extended to a spatial region which scales with the total volume V of the active medium.

The first condition also implies that the diagonal elements of $G_{k_1 k_2}$ are all equal and do not depend on the frequency. In particular, then, for a *strong cavity* and a regular medium these disappear from the equilibrium dynamics because of the spherical constraint.^{19,21}

The couplings are related to the spatial overlaps of the modes, cf. Eqs. (11)-(12), and are, therefore, not independent. However, in the mean-field limit off-diagonal correlations vanish for large system sizes and we can assume that the couplings are statistically independent.

Before discussing the properties of this solution we first rewrite the Hamiltonian in the mean-field form

$$\mathcal{H} = -\frac{1}{2} \sum_{jk}^{1,N} J_{jk} a_j a_k^* - \frac{1}{4!} \sum_{jklm}^{1,N} J_{jklm} a_j a_k a_l^* a_m^*, \quad (30)$$

where a_i are N complex amplitude variables subject to the spherical constraint $\sum_k |a_k|^2 = \mathcal{E}_0 \equiv \epsilon N$. The couplings J_{i_1, \dots, i_p} ($p = 2, 4$) are symmetric under index permutation and vanish if two or more indexes are equal. The non-null J_{i_1, \dots, i_p} are quenched independent identically distributed real random variables. In the mean-field limit only the first two moments are relevant, so we can take a Gaussian distribution:

$$\mathcal{P}(J_{i_1 \dots i_p}) = \frac{1}{\sqrt{2\pi\sigma_p^2}} \exp \left[-\frac{(J_{i_1 \dots i_p} - \tilde{J}_0^{(p)})^2}{2\sigma_p^2} \right]. \quad (31)$$

The requirement of an extensive Hamiltonian, i.e., proportional to N , requires that the variance and the average scale with N as

$$\sigma_p^2 = \frac{p! J_p^2}{2N^{p-1}}, \quad \tilde{J}_0^{(p)} = \frac{J_0^{(p)}}{N^{p-1}},$$

where J_p and $J_0^{(p)}$ are intensive parameters fixing the relative strength of various terms in the Hamiltonian. To have a direct interpretation in terms of optical quantities we express them as

$$J_0^{(4)} = \alpha_0 J_0, \quad J_0^{(2)} = (1 - \alpha_0) J_0, \quad (32)$$

$$J_4^2 = \alpha^2 J^2, \quad J_2^2 = (1 - \alpha)^2 J^2. \quad (33)$$

where the parameters J_0 and J fix the cumulative strength of the ordered and disordered part of the Hamiltonian, while α_0 and α the degree (i. e., relative strength)

of the non-linear quartic ($p = 4$) contribution in the ordered and disordered parts, respectively. Then we introduce the usual parameters of RL models: the *degree of disorder* R_J and the *pumping rate* \mathcal{P} as:²¹

$$R_J \equiv \frac{J}{J_0}, \quad \mathcal{P} \equiv \epsilon \sqrt{\beta J_0}, \quad (34)$$

where $\beta = T^{-1}$ is the ordinary inverse thermal bath temperature, cf. Eq. (17). The definition of the pumping rate encodes the experimental fact that the effect of decreasing the temperature of the bath or increasing the energy of the pump source is qualitatively the same on the onset of a random lasing regime.^{48,49} We stress that the effective “photonic” temperature $T_{\text{ph}} \equiv T/\epsilon^2$, coupled to \mathcal{H} in the Gibbs measure Eq. (29) in units of J_0 is nothing else than $\sqrt{\mathcal{P}}$.

With this parametrization the mean-field solution is conveniently expressed through the parameters

$$\begin{aligned} b_2 &= \frac{1 - \alpha_0}{4} \mathcal{P} \sqrt{\beta J_0}, & b_4 &= \frac{\alpha_0}{96} \mathcal{P}^2, \\ \xi_2 &= \frac{(1 - \alpha)^2}{4} \beta J_0 \mathcal{P}^2 R_J^2, & \xi_4 &= \frac{\alpha^2}{6} \mathcal{P}^4 R_J^2, \end{aligned} \quad (35)$$

which are the *photonics* counterpart of the standard p -spin-like¹⁶, or mode coupling theory like⁵⁰ parameters

$$\begin{aligned} b_2 &= \frac{\epsilon}{4} \beta J_0^{(2)}, & b_4 &= \frac{\epsilon^2}{96} \beta J_0^{(4)}, \\ \xi_2 &= \frac{\epsilon^2}{4} \beta^2 J_2^2, & \xi_4 &= \frac{\epsilon^4}{6} \beta^2 J_4^2, \end{aligned} \quad (36)$$

used in the statistical mechanics study of these type of models. Notice that, without loss of generality, in the standard parametrization ϵ can be fixed to any value by a suitable rescaling of the other parameters. Analogously, in the photonic parametrization, Eq. (35), the parameters can be rescaled to maintain βJ_0 fixed.

A. Statistical Mechanics of Quenched Disordered Systems

The couplings in the effective Hamiltonian (30) are extracted for an appropriate probability distribution and remain fixed - *quenched* - in the dynamics. Then the free-energy density $\phi_N[J]$, as any other observable, depends on the particular realization J of the disordered couplings. For a vast class of observables, including $\phi_N[J]$, however, the dependence disappears as the system becomes sufficiently large.¹⁴ Such property, called *self-averaging*, implies that

$$\lim_{N \rightarrow \infty} \phi_N[J] = \phi, \quad (37)$$

where ϕ does not depend on J and is equal to the thermodynamic limit $N \rightarrow \infty$ of the average of $\phi_N[J]$ over

the distribution $P[J]$ of J :

$$\begin{aligned} \phi &= \overline{\phi} = \lim_{N \rightarrow \infty} \int \mathcal{D}J P[J] \phi_N[J] \\ &= - \lim_{N \rightarrow \infty} \frac{1}{\beta N} \overline{\log Z_N[J]}. \end{aligned} \quad (38)$$

where

$$\begin{aligned} Z_N[J] &= \int \mathcal{D}a e^{-\beta \mathcal{H}[a, J]} \\ \mathcal{D}a &\equiv \prod_{k=1}^N da_k da_k^* \end{aligned} \quad (39)$$

The average of the logarithm of the partition function can be performed using the replica trick:^{14,51} one considers n copies of the system and evaluates the replicated partition function

$$\begin{aligned} \overline{Z_N^n} &= \int \mathcal{D}J P(J) \int \mathcal{D}a_1 \cdots \mathcal{D}a_n \\ &\times e^{-\beta [\mathcal{H}(a_1, J) + \dots + \mathcal{H}(a_n, J)]} \end{aligned} \quad (40)$$

as function of n . A continuation to real n is considered down to values $n < 1$, so that the free energy density is eventually obtained as the limit

$$\phi = - \lim_{N \rightarrow \infty} \lim_{n \rightarrow 0} \frac{1}{\beta N} \frac{\overline{Z_N^n} - 1}{n}. \quad (41)$$

The replicated partition function $\overline{Z_N^n}$ for large N , and fixed n , can be evaluated using the saddle-point method. Therefore, the thermodynamic limit $N \rightarrow \infty$ and the limit $n \rightarrow 0$ are essentially inverted in the evaluation. The mathematical foundations of the method are not simple and many efforts have been necessary to investigate this problem. In this scenario the well known Replica Symmetry Breaking scheme has been proposed by Parisi^{52,53} in the late 70's and rigorously proved by Guerra⁵⁴ and Talagrand⁵⁵ about 25 years later. This Ansatz solves the problem showing a distinctive picture of the underlying structure of the phase space⁵⁶ and, hence, conferring a key role to the replica trick.

B. Order Parameters in the Replica Formalism

To apply the replica method to the Hamiltonian (30) it is convenient to express first the complex mode amplitude a_j in term of its rescaled real and imaginary part, respectively σ_j and τ_j , as:

$$a_j = \sqrt{\epsilon} (\sigma_j + i\tau_j), \quad j = 1, \dots, N. \quad (42)$$

The spherical constraint then takes the form

$$\sum_{j=1}^N (\sigma_j^2 + \tau_j^2) = N \quad (43)$$

while the Hamiltonian (30) becomes

$$\mathcal{H} = -\epsilon \sum_{j < k} J_{jk} (\sigma_{jk} + \tau_{jk}) \quad (44)$$

$$- \epsilon^2 \sum_{j < k < l < m} J_{jklm} (\sigma_{jklm} + \tau_{jklm} + \varphi_{jklm}),$$

where we have introduced the short-hand notation

$$\sigma_{jk} \equiv \sigma_j \sigma_k$$

$$\sigma_{jklm} \equiv \sigma_j \sigma_k \sigma_l \sigma_m$$

and similarly for τ , and

$$\varphi_{jklm} = (\psi_{jk,lm} + \psi_{jl,km} + \psi_{jm,kl})/3$$

$$\psi_{jk,lm} = \sigma_{jk} \tau_{lm} + \sigma_{lm} \tau_{jk}.$$

In the limit of large N the replicated partition function averaged over the coupling probability distribution (31) can be written as an integral in the replica space of a functional of two matrices Q and R and two parameters m_σ and m_τ , details can be found in Appendix A:

$$\overline{Z_N^n} = \int \mathcal{D}Q \mathcal{D}R \mathcal{D}m_\sigma \mathcal{D}m_\tau e^{-NG[Q,R,m_\sigma,m_\tau]}, \quad (45)$$

where

$$-G[Q,R,m_\sigma,m_\tau] = \frac{1}{2} \sum_{a,b} g(Q_{ab}, R_{ab}) + n k(m_\sigma, m_\tau)$$

$$+ \frac{1}{2} \ln \det(Q + R) - \frac{m_\sigma^2}{2} \sum_{a,b} (Q + R)_{ab}^{-1} \quad (46)$$

$$+ \frac{1}{2} \ln \det(Q - R) - \frac{m_\tau^2}{2} \sum_{a,b} (Q - R)_{ab}^{-1}.$$

The sums over the replica indexes a and b run from 1 to n , and $g(x, y)$ and $k(x, y)$ are the two-variable functions:

$$g(x, y) = \xi_2(x^2 + y^2) + \frac{\xi_4}{2}(x^4 + y^4 + 4x^2y^2), \quad (47)$$

$$k(x, y) = b_2(x^2 + y^2) + b_4(x^2 + y^2)^2. \quad (48)$$

The matrices Q and R and m_σ and m_τ are related to the mode amplitudes by

$$Q_{ab} = \frac{1}{N} \sum_{j=1}^N (\sigma_j^a \sigma_j^b + \tau_j^a \tau_j^b) = \frac{1}{\mathcal{E}} \sum_{j=1}^N \text{Re}[a_j^a (a_j^b)^*] \quad (49)$$

$$R_{ab} = \frac{1}{N} \sum_{j=1}^N (\sigma_j^a \sigma_j^b - \tau_j^a \tau_j^b) = \frac{1}{\mathcal{E}} \sum_{j=1}^N \text{Re}[a_j^a a_j^b] \quad (50)$$

and⁵⁷

$$m_\sigma = \frac{\sqrt{2}}{N} \sum_{j=1}^N \sigma_j^a, \quad m_\tau = \frac{\sqrt{2}}{N} \sum_{j=1}^N \tau_j^a, \quad (51)$$

$$m_\sigma + i m_\tau = \frac{\sqrt{2}}{\mathcal{E}} \sum_{j=1}^N a_j^a. \quad (52)$$

These are the order parameters of the theory. The “magnetization” m_σ and m_τ are single replica quantities and cannot depend on the particular replica a because replicas are identical.

In the thermodynamic limit $N \rightarrow \infty$ the integral in the replica space can be evaluated using the saddle point method, leading to

$$\beta\phi = \beta\phi_0 + \lim_{n \rightarrow 0} \text{Extr} \frac{1}{n} G[R, Q, m_\sigma, m_\tau] \quad (53)$$

where ϕ_0 is an irrelevant constant. The functional $G[Q, R, m_\sigma, m_\tau]$ must be evaluated at its stationary point that, as $n \rightarrow 0$, gives the maximum with respect to variations of Q and R and the minimum with respect to variations of m_σ and m_τ .

To find the stationary point of $G[Q, R, m_\sigma, m_\tau]$ an ansatz on the structure of the matrices Q and R is necessary. It turns out that the simplest ansatz of assuming $Q_{ab} = Q$ and $R_{ab} = R$ for all $a \neq b$, i.e., of assuming that all replicas are equivalent under pair exchange, is not thermodynamically stable in the whole phase space, specifically at low temperature/high power. Therefore, one must allow for a spontaneous Replica Symmetry Breaking (RSB) and construct the solution accordingly. Following the Parisi scheme,¹⁴ a $n \times n$ matrix M in a \mathcal{R} -step RSB state⁵⁸ is described by $\mathcal{R} + 2$ parameters ($M_{\mathcal{R}+1}, M_{\mathcal{R}}, \dots, M_0$) by dividing it along the diagonal into blocks of decreasing linear size p_r , with $1 = p_{\mathcal{R}+1} < p_{\mathcal{R}} < \dots < p_0 = n$, and assigning $M_{ab} = M_r$ if the replicas a and b belong to the same block of size p_r but to two distinct blocks of size p_{r+1} .

Introducing the σ and τ overlap matrices A and B

$$A_{ab} = Q_{ab} + R_{ab} = \frac{2}{N} \sum_{j=1}^N \sigma_j^a \sigma_j^b,$$

$$B_{ab} = Q_{ab} - R_{ab} = \frac{2}{N} \sum_{j=1}^N \tau_j^a \tau_j^b, \quad (54)$$

the functional G for a generic \mathcal{R} -RSB solution is conveniently written as

$$-2G = \sum_{r=0}^{\mathcal{R}+1} (p_r - p_{r+1}) g(Q_r, R_r) \quad (55)$$

$$+ 2k(m_\sigma, m_\tau) - \frac{m_\sigma^2}{A_0} - \frac{m_\tau^2}{B_0}$$

$$+ \log(A_{\mathcal{R}+1} - A_{\mathcal{R}}) + \sum_{r=1}^{\mathcal{R}+1} \frac{1}{p_r} \log \frac{A_{\widehat{r}}}{A_{\widehat{r+1}}} + \frac{A_0}{A_1}$$

$$+ \log(B_{\mathcal{R}+1} - B_{\mathcal{R}}) + \sum_{r=1}^{\mathcal{R}+1} \frac{1}{p_r} \log \frac{B_{\widehat{r}}}{B_{\widehat{r+1}}} + \frac{B_0}{B_1},$$

where the hatted quantities are the Replica Fourier Transform (RFT) of a \mathcal{R} -RSB matrix M_r defined as^{59–61}

$$\begin{aligned} M_{\hat{k}} &= \sum_{r=k}^{\mathcal{R}+1} p_r (M_r - M_{r-1}) \\ M_r &= \sum_{k=0}^r \frac{1}{p_k} \left(M_{\hat{k}} - M_{\widehat{k+1}} \right), \end{aligned} \quad (56)$$

where it is intended that terms with indices outside the respective interval of definition are null.

The solutions of the stationarity equations, see Appendix B, are either of the form

$$m_\tau = 0 \text{ and } B_r = 0 \rightarrow R_r = Q_r, \quad r = 0, \dots, \mathcal{R}, \quad (57)$$

or (because of the symmetry $\sigma \leftrightarrow \tau$):

$$m_\sigma = 0 \text{ and } A_r = 0 \rightarrow R_r = -Q_r, \quad r = 0, \dots, \mathcal{R}. \quad (58)$$

In the following, without loss of generality, we consider the first form, Eq. (57), and, for simplicity, we drop the subscript in the magnetization writing $m_\sigma = m$.

III. OPTICAL REGIMES AND PHASE DIAGRAM

The phase diagram obtained from the analysis of the solution of the mean-field model consists of four different phases distinguished by the values of the order parameters Q , R and m :

- *Incoherent Wave (IW)*: replica symmetric solution with all order parameters equal to zero. The modes oscillate incoherently in this regime and the light is emitted in the form of a continuous wave. At low pumping, else said high temperature, this is the only solution. It corresponds to the Paramagnetic phase in spin models.
- *Standard Mode-Locking Laser (SML)*: solutions with $m \neq 0$, with or without replica symmetry breaking. The modes oscillate coherently with the same phase and the light is emitted in form of optical pulses. It is the only regime at high pumping (low temperature) when b_2 and b_4 are large with respect to ξ_2 and ξ_4 , that is when the degree of disorder R_J is small. It corresponds to the Ferromagnetic phase in spin models.
- *Random Laser (RL)*: the modes do not oscillate coherently in intensity, so that $m = 0$, but $R_{aa} = \langle \sigma^2 \rangle - \langle \tau^2 \rangle \neq 0$ implying a phase coherence and the overlap matrices have a nontrivial structure. It is the only phase in the high pumping limit for large disorder, i.e., when ξ_2 and ξ_4 are large with respect to b_2 and b_4 . It corresponds to the Spin Glass phase in spin models with disordered interactions.

- *Phase Locking Wave (PLW)*: all order parameters vanish but R_{aa} , so that $\langle \sigma^2 \rangle \neq \langle \tau^2 \rangle$, signaling a locking of the mode phases in a specific direction. This regime occurs in a region of the phase space intermediate between the IW and RL regimes if $\xi_4 > 0$ ($R_J > 0$). This new thermodynamic phase, to our knowledge never observed in spin models, follows from the peculiar kind of spins considered, displaying both a phase and a magnitude, that leads to a combination of XY (only phase) and real spherical (only magnitude) spins. The locking in the two degrees of freedom of each complex amplitude does not happen concurrently as the temperature is lowered in presence of (even a small amount of) disorder. Mode phases lock first, in what we call the PLW regime.

The narrow band approximation, in which the present model is exact, makes the study of the pulsed emission particularly delicate. Indeed, if the magnetization is nonzero, as in the SML phase, the light is generated in form of short pulses when the presence of different frequencies in the spectrum is considered and this property cannot be reproduced in the narrow-band limit. Besides, we note that a ML phase with a nonzero phase delay, as described in Ref. [62 and 63], associated with pulsed emission in an unmagnetized state is not feasible, as the frequency does not play any role in the mode evolution. Nevertheless, it is possible to analytically solve the model in the whole phase diagram and describe all regimes for optically active media.

Different replica symmetry breaking solutions, and corresponding RL regimes, occur by varying the ratio $r \equiv \xi_2/\xi_4$, or, equivalently, varying the strength of disordered nonlinearity α . In particular, for r large enough (α small enough) the stable thermodynamic phase is expected to be characterized by a Full Replica Symmetry Breaking (FRSB) state.³⁷ In realistic optical systems the 2-body interaction is usually not dominant above the lasing threshold, cf. discussion in Sect. I. However, there can be systems where the damping due to the openness of the cavity is strong enough to compete with the nonlinearity and a FRSB state may emerge. In this case the transition turns out to be continuous in the order parameters: the overlap is zero at the critical point and grows continuously as the power is increased above threshold. In this work we shall limit ourselves to the analysis of the first step of replica symmetry breaking, by considering solutions with only one step of replica symmetry breaking (1RSB). We, hence, provide the exact mean-field laser solution for r low enough (specifically, $r < 0.517$ for $b_2 = b_4 = 0$). Due the continuous nature of the transition to the FRSB regime, though, the 1RSB solution is also a reliable approximation of the lasing solution not far from threshold for larger r .

A. RS and 1RSB phases

Solutions with non-null magnetization m originates because of the ordered, non-random, part of the Hamiltonian. These are more easily described by introducing a suitable external field h and considering the fully-disordered model, i.e., with $J_0^{(p)} = 0$, with Hamiltonian

$$\mathcal{H}_h = \mathcal{H} - \sqrt{2}h \sum_j \sigma_j, \quad (59)$$

where \mathcal{H} is given in (44) and, the $\sqrt{2}$ follows from the definition (51) of m_σ . Absorbing the factor β into the field writing $b = \beta h$, the solutions of the two models are identical provided

$$b = \frac{\partial}{\partial m} k(m, 0), \quad (60)$$

so that we have the *unfolding equation*

$$b = (2b_2 + 4b_4 m^2) m, \quad (61)$$

which relates the $m \neq 0$ states of the original model (30) to the ones of model (59). For the solution with $m_\sigma = 0$ and $m_\tau = m$ there is an equivalent mapping. The origin of this connection is discussed in Appendix B. Note that for $b \neq 0$ all solutions have $m \neq 0$, and hence correspond to the SML regime. The other phases with $m = 0$ correspond to the $b = 0$ case. The appearance of nontrivial solutions of the unfolding equation (61) then signals the transition to the SML regime.

The parameterization $a \rightarrow (\sigma, \tau)$ given in (42) ensures that the diagonal elements Q_{aa} are equal to 1. The diagonal elements of R_{aa} are also independent from the replica index a but the value depends on the control parameters. The analysis of the solution (57) is then simplified by introducing the “scaling factor”

$$\bar{a} = Q_{aa} + R_{aa} = 1 + R_{\mathcal{R}+1}, \quad (62)$$

varying between 1 and 2, and using the rescaled overlap parameters q_r defined as

$$Q_r + R_r = 2Q_r = \bar{a} q_r, \quad r = 0, \dots, \mathcal{R}. \quad (63)$$

For the solution (58) one has a similar parameterization.

In this work we shall only consider solutions with $\mathcal{R} = 0$ (RS) and $\mathcal{R} = 1$ (1RSB). The study of solution with more complex RSB structure will not be reported here.

The RS solution is described by the three parameters q_0 , \bar{a} and m and, neglecting all unnecessary terms, the free energy functional (53) reads:

$$2\beta\phi(q_0, \bar{a}, m) = -\bar{g} + g_0 - \frac{q_0 - m^2/\bar{a}}{1 - q_0} - \log[\bar{a}(2 - \bar{a})(1 - q_0)] - 2bm, \quad (64)$$

where we have used the short-hand notation:

$$\begin{aligned} \bar{g} &= g(1, \bar{a} - 1), \\ g_r &= g\left(\frac{\bar{a}}{2} q_r, \frac{\bar{a}}{2} q_r\right). \end{aligned} \quad (65)$$

Stationarity of $\phi(q_0, \bar{a}, m)$ with respect to variation of q_0 , \bar{a} and m leads to the stationary equations:

$$\begin{aligned} \bar{a} \Lambda_0 &= \frac{q_0}{(1 - q_0)^2} - \bar{a} b^2, \\ \bar{a} \bar{\Lambda} - \bar{a} \Lambda_0 &= -\frac{1}{1 - q_0} + \frac{\bar{a}}{2 - \bar{a}}, \end{aligned} \quad (66)$$

and $m = b\bar{a}(1 - q_0)$, where

$$\begin{aligned} \bar{\Lambda} &= \Lambda(\bar{a} - 1, 1), \\ \Lambda_r &= \Lambda\left(\frac{\bar{a}}{2} q_r, \frac{\bar{a}}{2} q_r\right), \end{aligned} \quad (67)$$

with

$$\Lambda(x, y) = \frac{\partial}{\partial x} g(x, y) = 2x [\xi_2 + \xi_4 (x^2 + 2y^2)]. \quad (68)$$

The 1RSB solution requires five parameters: q_0 , q_1 , \bar{a} , m and the “block size” p_1 . The latter becomes a real number for $n \rightarrow 0$, the RSB parameter $p_1 = x \in [0, 1]$. The free energy for the 1RSB solution then reads:

$$\begin{aligned} 2\beta\phi(q_0, q_1, x, \bar{a}, m) &= -\bar{g} + (1 - x)g_1 + xg_0 \\ &\quad - \frac{q_0 - m^2/\bar{a}}{q_1} - \log[\bar{a}(2 - \bar{a})(1 - q_1)] \\ &\quad - \frac{1}{x} \log \frac{q_1}{q_2} - 2bm, \end{aligned} \quad (69)$$

where

$$q_2 = 1 - q_1, \quad q_{\bar{1}} = 1 - q_1 + x(q_1 - q_0). \quad (70)$$

Stationarity of the functional with respect to variations of q_0 , q_1 , \bar{a} , m gives the stationarity equations:

$$\begin{aligned} \bar{a} \Lambda_0 &= \frac{q_0}{q_1^2} - \bar{a} b^2, \\ \bar{a} \Lambda_1 - \bar{a} \Lambda_0 &= \frac{q_1 - q_0}{q_2 q_{\bar{1}}}, \\ \bar{a} \bar{\Lambda} - \bar{a} \Lambda_1 &= -\frac{1}{1 - q_1} + \frac{\bar{a}}{2 - \bar{a}}, \\ m &= \bar{a} b q_{\bar{1}}. \end{aligned} \quad (71)$$

The role of the parameter x is more subtle. If the free energy functional is required to be stationary also with respect to variations of x , one then obtains the additional stationarity equation:

$$\begin{aligned} g_1 - g_0 &= -\frac{1}{x^2} \log \frac{q_2}{q_{\bar{1}}} \\ &\quad - (q_1 - q_0) \left[\frac{1}{x q_{\bar{1}}} - \frac{q_0 - m^2/\bar{a}}{q_{\bar{1}}^2} \right], \end{aligned} \quad (72)$$

which describes the *static* solution with null complexity, see Sect. III C for more detail. This equation can be rewritten, making use of the other Eqs. (71), as

$$2 \frac{g_1 - g_0 - \bar{a} \Lambda_0 (q_1 - q_0)}{\bar{a} (\Lambda_1 - \Lambda_0) (q_1 - q_0)} = z(y), \quad (73)$$

where $y = q_2/q_1 \in [0, 1]$ and

$$z(y) = -2y \frac{1 - y + \ln y}{(1 - y)^2}, \quad (74)$$

is the CS z -function.¹⁶ This form is particularly useful for the numerical solution of the stationary equations, in particular to find solutions for fixed value of x (that is, along a x -line). Note also that it depends only on the ratio $r = \xi_2/\xi_4$ and not on ξ_2 and ξ_4 separately.

Alternatively, the value of x can be fixed by requiring that the complexity, i.e., the number of equivalent metastable states - or ergodic components - is maximal. This choice leads to the *dynamic* solution, and to the following equation for x :

$$\left[\frac{\partial}{\partial x} + \frac{\partial}{\partial y} \right] \Lambda(x, y) \Big|_{x=y=\bar{a}q_1/2} = \frac{2}{\bar{a}^2 (1 - q_1)^2}. \quad (75)$$

We defer a more detailed discussion to Sect. III C.

The analysis of the solutions can be done in two steps. First we discuss the solutions in presence of a fixed field $b = \beta h$. Then, once the different phases have been identified, we shall *unfold* b in terms of m using the unfolding equation to recover the original RL problem. For this reason the phase diagrams will be reported in the (ξ_2, ξ_4, b) , (ξ_2, ξ_4, b_2, b_4) and $(\mathcal{P}, \alpha, \alpha_0, R_J)$ spaces, as appropriate. The relation among the different spaces are given in Eqs. (35) and the unfolding equation (61).

B. Phase Diagram at Fixed Field

To study the transition to the RL state we consider first the case of zero external field h . The complete phase diagram for $b = 0$, including phases with RSB structure more complex than RS or 1RSB, is shown in Figs. 1 and 2. In particular, the IW is the only phase at high enough temperature. Lowering the temperature, for $\xi_4 > 0$, the IW becomes metastable as the PLW phase appears continuously. The case of $\xi_4 = 0$ is different: increasing ξ_2 the IW phase becomes unstable and a transition occurs to replica symmetric RL phase.

For $r = \xi_2/\xi_4 < 0.517$, i.e., $\alpha > \alpha_{nl} \simeq (3 - 1.76382\epsilon)(3 - 1.03703\epsilon^2)^{-1}$, increasing ξ_4 the PLW regime undergoes a Random First Order Transition (RFOT)⁴² to a glassy RL phase with 1RSB: a jump is present in the order parameters Q and R but the internal energy remains continuous. Thus, no latent heat is exchanged.

For $r = \xi_2/\xi_4 > 0.517$ the PLW becomes unstable at a critical temperature where the transition occurs to a RL regime with FRSB, of the kind reported in Ref. [37].

The complete phase diagram at non-zero external field is shown in Fig. 3. In this case it is useful to introduce the ratio $t = q_0/q_1 \in [0, 1]$. The 1RSB solutions can be found fixing the parameters r, x, t and using the stationary point equations to find the value of ξ_4, b, y and \bar{a} . Two surfaces are of particular interest: the surface $x = 1$, corresponding to the RFOT between the RS

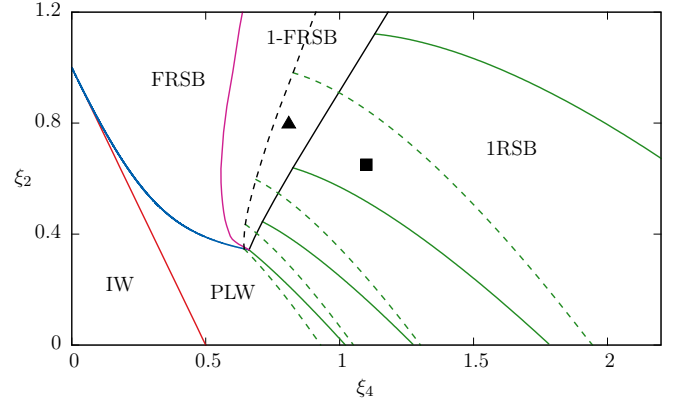


FIG. 1. Phase diagram ξ_2, ξ_4 for $b = 0$ with static (solid green) and dynamic (dashed green) x -lines. In the 1RSB phase, x -lines with different value of x are shown both in the static and dynamic cases: $x = 0.45, 0.6, 0.8$ and $x = 1$ top to bottom. The $x = 1$ static x -line is the static glassy RFOT line between the PLW phase and the RL with 1RSB phase. The $x = 1$ dynamic x -line is where the dynamics arrests because of the exponential number of metastable states characteristic of the RFOT. The solid black line marks the end point of the x -lines and a 1-FRSB appears. The dashed black line is the analogous critical line of dynamic x -lines. Both static and dynamic 1-FRSB phases end on the solid magenta line. Here the complexity vanishes and a transition to a FRSB phase occurs. Finally the solid blue line marks the direct transition between the PLW and the FRSB phases. The order parameters are continuous crossing this line. The \blacksquare and \blacktriangle symbols correspond to the positions of the data shown in Fig. 5.

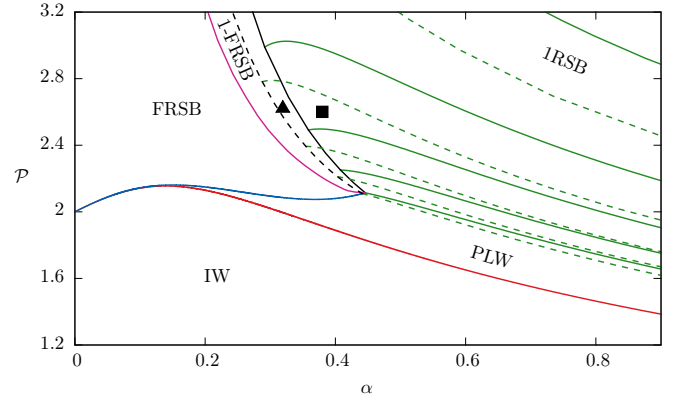


FIG. 2. Phase diagrams for $b = 0$ in the photonic parameters, pumping rate \mathcal{P} and degree of openness α , for $R_J = \beta J_0 = 1$.

and 1RSB solution (Fig. 3: green surface), and the surface $t = 1 \leftrightarrow q_0 = q_1$ corresponding to the continuous transition between the RS and RSB phase (Fig. 3: red surface).

A condition for the existence of the 1RSB solution can be derived considering the stationarity equations for t close to 1. In this case the ratio $w \equiv (1 - t)/(1 - y)$ has

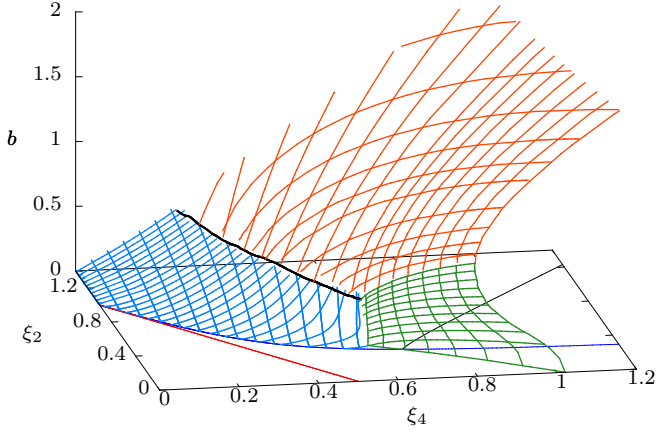


FIG. 3. Phase diagram of the 2 + 4 complex spherical model at fixed external field in the (ξ_2, ξ_4, b) space. Only the static solution is shown. The green surface, given by the 1RSB solution with $x = 1$, is the critical RFOT surface between the RS and 1RSB phases. The red surface, given by the 1RSB solution with $t = 1 \rightarrow q_1 = q_0$, gives critical surface of the continuous transition between the RS and 1RSB phases. The black line marks the end-line of the 1RSB solution. The blue surface is critical surface where the (continuous) transition between the RS to FRSB phases occurs.

the finite limit

$$w = -\frac{-9\bar{a}^2 + 8rx + 3\sqrt{9\bar{a}^4 - 16\bar{a}^2rx^2 - 16\bar{a}^2rx}}{8rx^2}.$$

as $t \rightarrow 1$ and $y \rightarrow 1$ simultaneously. The 1RSB solution thus exist only if

$$16rx(x+1) \leq 9\bar{a}^2.$$

This critical line is drawn in black in Fig. 3. Since the condition becomes more and more stringent increasing x , this line does not exist for $r < 9/32$. The line lies on the RS instability surface, drawn in blue in Fig. 3, where the eigenvalue

$${}_2\Lambda(0; 1, 1) = -2\xi_2 - \frac{9}{2}\xi_4\bar{a}^2q_0^2 + \frac{2}{\bar{a}^2(1-q_0)^2}, \quad (76)$$

of the fluctuations about the RS saddle point, with \bar{a} and q_0 are evaluated at RS saddle point (66), vanishes. The eigenvalue can be computed by extending the calculation of Appendix D to the case $Q_0 \neq 0$. Alternatively it can be derived from the 1RSB stability analysis of Appendix E by setting $x = 0$ and replacing Q_1 of the 1RSB solution with Q_0 of the RS solution. The eigenvalue (76) then follows from (E7).

As for the zero-field case, the RS solution is stable in the whole phase space. For high r the 1RSB solution disappears for values of x smaller than a threshold value that decreases as r increases and it is replaced by a FRSB solution, as it occurs for real spherical spin models.³⁷

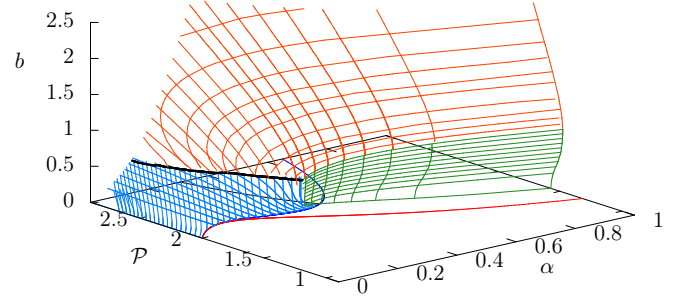


FIG. 4. Same as in Fig. 3 in the photonic (\mathcal{P}, α, b) diagram.

C. Complexity

Looking at Fig. 1 one sees that when $b = 0$ and $r = \xi_2/\xi_4 < 0.517$ the static transition line, the solid 1-line, from the PLW to the RL regime is anticipated by a dynamic transition line, dashed 1-line. Approaching this line from the PLW side a critical slowing down, followed by a dynamic arrest on the line, is observed in the time correlation functions. This behavior, typical of glassy systems, is due to the breaking of ergodicity of the phase space. The phase space breaks down into a large number \mathcal{N} , increasing *exponentially* with the size of the system, of degenerate metastable states that dominate the dynamical behavior before the true thermodynamic (static) transition is reached, see, e.g., Refs. [15], [64] and [50].

Lasing in random media is hence expected to display a *glassy* coherent behavior. With glassy we mean that (i) a sub-set of modes out of an extensive ensemble of localized passive modes are activated in a non-deterministic way and (ii) the whole set of activated modes behaves cooperatively and belongs to one state out of (exponentially) many possible ones. We stress that in characterizing the glassy behavior, by *non-deterministic* we do not mean deterministic chaos, i.e., high sensitivity to initial conditions. Chaos is, actually, a dynamic phenomenon occurring in laser systems,⁶⁵ but it is independent from possible glassy properties. In other words, chaos can occur in these systems, but it does not affect the presence or absence of glassiness, as, e.g., shown in Ref. [66]: it is not a necessary nor a sufficient feature for random lasers.

The role of the metastable states can be captured by introducing the *complexity*, aka *configurational entropy*,

$$\Sigma \equiv \frac{1}{N} \log \mathcal{N}. \quad (77)$$

The complexity Σ as function of the free energy of the metastable states can be obtained from the Legendre transform of $\phi(x)$:^{67–69}

$$\Sigma(f) + \beta x \phi(x) = \beta x f, \quad (78)$$

$$f = \frac{\partial x \phi(x)}{\partial x} \quad (79)$$

where f is the free energy of a single metastable state and $x = x(f)$ is the solution of Eq. (79).

When $h = 0$ the overlap q_0 vanishes and the 1RSB free energy functional (69) evaluated on the stationary point (71) reduces to:

$$2\beta\phi(x) = -\bar{g} + (1-x)g_1 - \log[\bar{a}(2-\bar{a})(1-q_1)] - \frac{1}{x} \log \frac{q_1}{q_2}, \quad (80)$$

which replaced into the Legendre transform (78), yields

$$\Sigma = \frac{\beta}{2} \left[-\frac{q_1 x}{q_1} - g_1 x^2 + \ln \frac{q_1}{q_2} \right], \quad (81)$$

where $q_1 = q_1(x)$. To obtain the complexity $\Sigma(f)$ one should replace $x = x(f)$ or, alternatively, use x or q_1 as a free parameter and evaluate f from Eq. (79).

Stationarity of $\Sigma(f) - \beta x f$ with respect to variation of f for fixed x leads to $x = \beta^{-1}(\partial/\partial f)\Sigma(f)$. Physically acceptable solutions f must have $x \in [0 : 1]$ and, hence, $\Sigma(f)$ is a non-decreasing function of f .

The static solution corresponds to the metastable states with the lowest free energy and null complexity, i. e., the lowest acceptable value of Σ . For these states $f = \phi$ and from Eq. (79) one easily recovers the static stationary condition $\partial_x \phi(x) = 0$. The dynamical behavior of the system is dominated by the large number of metastable states with the highest physically acceptable free energy f , for which the complexity reaches its maximum value.

The range of allowable f is fixed by stability condition of the saddle point replica calculation, i.e., that the two relevant eigenvalues, see Appendix E:

$${}_1\Lambda(0; 1, 1) = -2\xi_2 + \frac{2}{\bar{a}^2[1 - q_1(1-x)]^2}, \quad (82)$$

$${}_1\Lambda(1; 2, 2) = -2\xi_2 - \frac{9}{2}\xi_4\bar{a}^2q_1^2 + \frac{2}{\bar{a}^2(1-q_1)^2}, \quad (83)$$

of the fluctuations about the 1RSB saddle point are non-negative. The eigenvalue ${}_1\Lambda(0; 1, 1)$ controls the fluctuations with respect to $q_0 = 0$ and its vanishing marks the end of the 1RSB phase and the appearance of a 1-FRSB phase.^{70,73} The eigenvalue ${}_1\Lambda(1; 2, 2)$ controls the stability with respect to fluctuations of q_1 . It can be shown that it also controls the critical slowing down of the dynamics,⁷¹ and, hence, its vanishing leads to the *marginal condition* for the arrested dynamics. The requirement of a maximal complexity is then equivalent to ${}_1\Lambda(1; 2, 2) = 0$, cf. Eq. (75).

In Fig. 5 the form of $\Sigma(q_1)$ is shown for two representative cases. In the upper panel only the dynamic 1RSB solution exists. The minimum $\Sigma = 0$ lies indeed outside the stability region of the 1RSB phase and the static 1RSB solution is unstable. Here the static solution is replaced by a solution with a more complex RSB structure, namely a 1-FRSB phase.

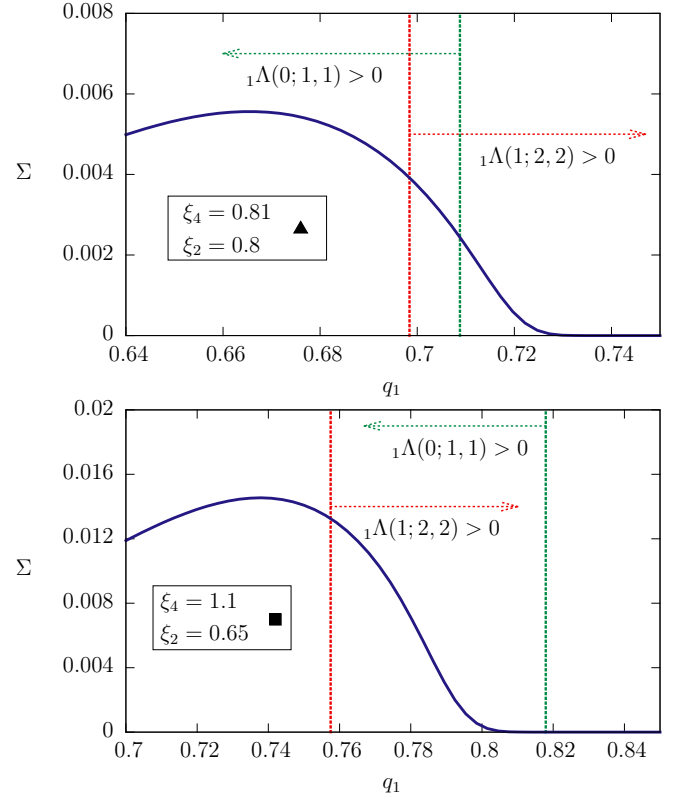


FIG. 5. Complexity Σ (blue solid line) as function of q_1 for $\xi_4 = 0.81$, $\xi_2 = 0.8$ (upper panel, \blacktriangle symbol in Fig. 1) and $\xi_4 = 1.1$, $\xi_2 = 0.65$ (lower panel, \blacksquare symbol in Fig. 1). The red dashed line indicates the region where the eigenvalue ${}_1\Lambda(1; 2, 2)$ is positive. The green dashed line indicates the region where the eigenvalue ${}_1\Lambda(0; 1, 1)$ is positive. The interval of q_1 where they are both positive identify the region where the 1RSB solution is stable for the given ξ_2, ξ_4 . In the upper panel the static 1RSB solution is unstable, $\Sigma = 0$ lies outside the allowed region, and only the dynamic 1RSB solution exists. The static solution here exists but with a more complex RSB structure.

Decreasing ξ_2 reduces the stability region of the 1RSB solution and eventually also the dynamic 1RSB solution becomes unstable. This occurs on the dashed black line shown in in Fig. 1. Beyond this line only a 1-FRSB phase, both static and dynamic, exists. We shall not enter into the detail of this phase, it is enough to say that, as it occurs for the 1RSB phase, they differ in complexity. A further decrease of ξ_2 reduces the complexity of the dynamic solution and it eventually vanishes when the magenta solid line is reached. Here the distinction between static and dynamic solution disappears and both solutions merge into a FRSB state.

D. Unfolding the field

In the low temperature phase all solutions with null external field b described so far belong to the SML phase

$m \neq 0$, since $m = b\bar{a}q_1$. The description of the SML phase in terms of b is then trivial. To switch to the description in terms of the parameters b_2 and b_4 , cf. Eq. (36), we have to unfold the value of the field b in terms of b_2 and b_4 using the *unfolding equation* (61). The unfolding equation admits the trivial solution $m = 0$ and a non-trivial $m \neq 0$ solution if

$$2b_2 + 4b_4m^2 = \frac{1}{\bar{a}q_1}. \quad (84)$$

The SML phase exists only in the regions of the phase space where this condition is satisfied. As in ordinary ferromagnetic first order transition, the SML phase may appear discontinuously with a finite value of m and higher free energy on the spinodal line. If this happens the SML phase becomes thermodynamically favorable only when the SML free energy becomes equal to the free energy of the $m = 0$ solution. This condition defines the transition line in the phase space. Since the two phases have equal free energy at the transition they coexist and latent heat is exchanged during the transition.

Using the stationary point equations (71) and defining $\gamma = b_2/b_4$, from Eq. (84) one easily gets:

$$b_4 = \frac{1}{\bar{a}q_1} \frac{1}{2\gamma + 4b^2\bar{a}^2q_1}, \quad (85)$$

which relates the value of b_4 for fixed γ to the that of the parameters of the model with fixed b . With this parametrization the SML spinodal line corresponds to the minimum values of b_4 where the $m \neq 0$ solution first appears. Since when $m = 0$ the field b vanishes and consequently $q_0 = 0$, it is useful to use q_0 as free parameter in the model with fixed b . The SML spinodal line for fixed γ then occurs at $b_4^* = \min_{q_0} b_4(q_0)$. The value of b_4^* is strictly positive, and a rough estimate gives the bound:

$$b_4^* \geq [2(1 + \mathcal{R})(\gamma + 2\epsilon)]^{-1}.$$

Note that the bound decreases with the number of steps \mathcal{R} of RSB, thus SML phases with higher replica symmetry breaking steps appear first, if they exists. In the following we shall only discuss the RS SML phase with $\mathcal{R} = 0$. While the discussion of SML phases with more complex RSB structures, though feasible, will not be presented here.

For large values of γ the minimum of $b_4(q_0)$ occurs at $q_0 = 0$ and the SML appears continuously with $m = 0$. The spinodal line then coincides with the transition line and the transition between the IW/PWL and SML phases is continuous in m , with no phase coexistence and latent heat.

For sufficiently small γ the minimum of $b_4(q_0)$ moves to $q_0 > 0$ and the SML phase appears discontinuously with $m \neq 0$. Thermodynamic transitions between the IW or PWL phases and the SML phase occur at the critical value $b_4^* > b_4^*$ where the free energy of the phases becomes equal.

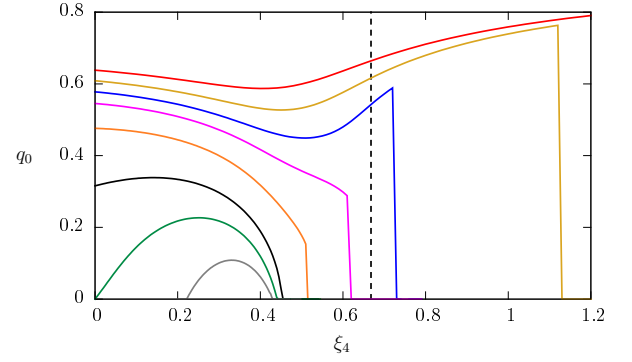


FIG. 6. Curves of q_0 where $b_4(q_0)$ is minimal as function of ξ_4 for fixed γ and $r = 0.5$. Bottom to top: $\gamma = 10^3, 4, 2.5, 1.5, 1, 0.75, 0.5, 0.25$. The vertical dashed line marks the value $\xi_4 \simeq 0.67$ where the 1RSB solution for $r = 0.5$ appears. For γ small enough the spinodal line of the RS SML phase enters into the 1RSB region.

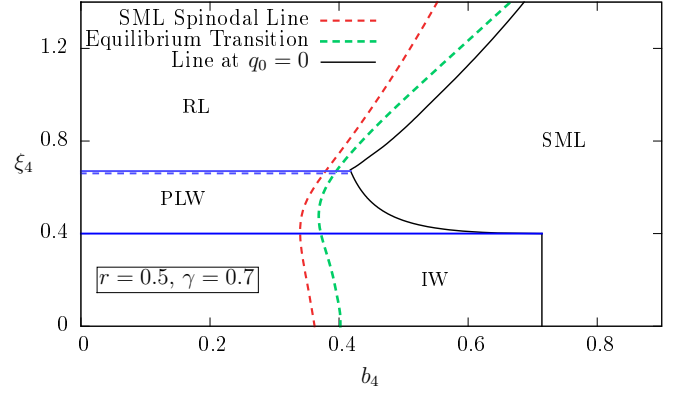


FIG. 7. Phase diagram for the model with $r = 0.5$ and $\gamma = 0.7$. For this value of γ the spinodal line of the RS SML phase enters into the 1RSB region. Dashed red line: spinodal line of the RS SML phase. Dashed green line: thermodynamic transition line. Solid black line: $b_4(q_0 = 0)$ line. Horizontal lines: transition lines between the $m = b = 0$ phases.

In Fig. 6 the value of q_0 is shown at which $b_4(q_0)$ attains its minimum as a function of ξ_4 for different values of γ . In figure 6 it is $r = 0.5$ but the scenario remains qualitative the same by changing r .

In Fig. 7 we report the phase diagram for $r = 0.5$ and $\gamma = 0.7$ in the plane (b_4, ξ_4) . Similarly, in Fig. 8 it is shown the phase diagram for $r = \gamma = 0$ when only the 4-body interaction term is present. In this latter case as $\xi_4 \rightarrow 0$ the transition occurs at $b_4^c = 0.613852$, green dashed line in Figure 8, in agreement with the result of Ref. [43] ($b_4 = \gamma_s P_0^2 / (12T)$ in the units of Ref. [43]).

The unfolding can be also done using the photonics parameters. The procedure is conceptually similar but

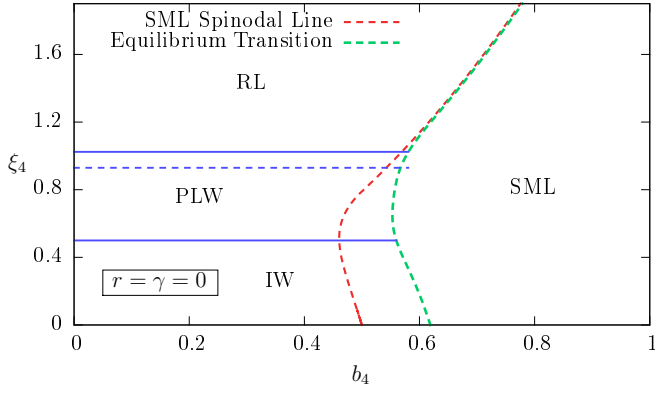


FIG. 8. Phase diagram for the model with $r = \gamma = 0$. Dashed red line: spinodal line of the RS SML phase. Dashed green line: thermodynamic transition line. Solid black line: $b_4(q_0 = 0)$ line. Horizontal lines: transition lines between the $m = b = 0$ phases.

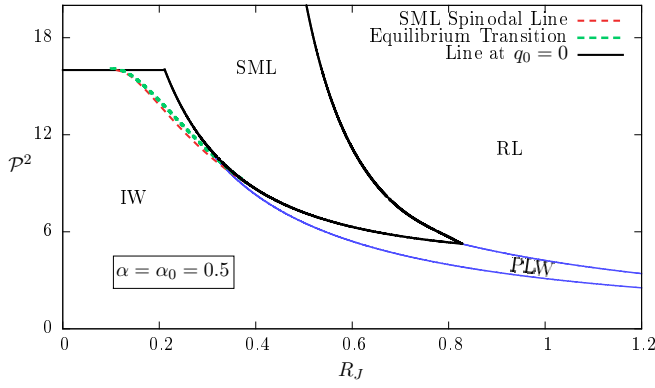


FIG. 9. Phase diagram in the photonics parameters for $a = a_0 = 0.5$. Dashed red line: spinodal line of the RS SML phase. Dashed green line: thermodynamic transition line. Solid black line: $b_4(q_0 = 0)$ line. Blue lines: transition lines between the $m = 0$ phases. The transition between the PLW and RL phases is continuous with null complexity.

more involved because the unfolding equation is now:

$$b = \frac{1}{2} \mathcal{P} \sqrt{\beta J_0} \left[1 + \left(\frac{\mathcal{P}}{12\sqrt{\beta J_0}} m^2 - 1 \right) \alpha_0 \right] m. \quad (86)$$

Regardless of which approach one uses, this procedure allows to obtain the phase diagram for general values of the photonic control parameters, which eventually may be compared in experimental setups; see, in particular, Ref. [72].

As an example, in Figs. 9-11 we show the phase diagram in the photonic parameters for $\alpha = \alpha_0 = 0.5, 0.7$ and 1. For $\alpha = \alpha_0 = 1$ only the 4-body interaction term is present, corresponding to the limit of ideally closed cavity. The transition from IW to SML is discontinuous, first order, as α_0 is large.

Consider the common experimental situation where we

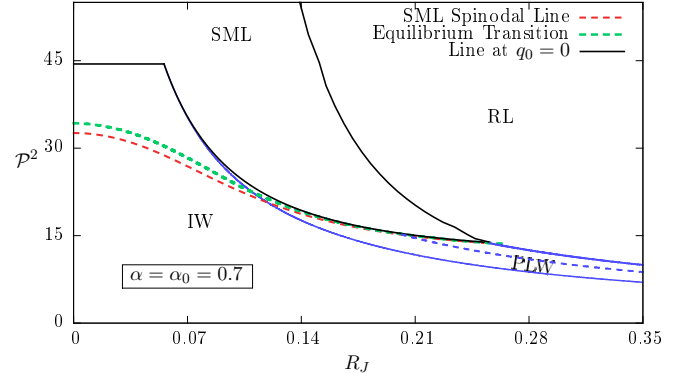


FIG. 10. Phase diagram in the photonics parameters for $a = a_0 = 0.7$. Dashed red line: spinodal line of the RS SML phase. Dashed green line: thermodynamic transition line. Solid black line: $b_4(q_0 = 0)$ line. Blue lines: transition lines between the $m = 0$ phases. The dashed blue line is the dynamic transition with finite complexity.

have an increasing pumping rate \mathcal{P} for fixed degree disorder R_J , α and α_0 . Then:

- For R_J not too large a direct transition between the IW and the SML phases is observed as the pumping increases. The transition is robust with respect to the introduction of a small amount of disorder;
- for systems with intermediate disorder, the high pump regime remains the ordered SML regime, but an intermediate unmagnetized, phase-coherent PLW regime appears between SML and IW regime;
- for large R_J , a further transition from the SML to the RL phase is observed at high \mathcal{P} . Moreover, if R_J exceeds a disorder threshold the SML disappears and the only high pumping lasing phase remains the RL.

This scenario is rather general and remains valid for different choices of α and α_0 . See for example Fig. 12 where the whole phase diagram for the case $\alpha = \alpha_0$ is reported. The global picture, however, does not change using different values of the ratio α/α_0 .

In general, the value of α_0 affects the transition toward the ordered SML regime: for high α_0 the transition is always first order. In particular, in the standard closed cavity laser limit $\alpha_0 = 1$ and no disorder ($R_J = 0$).⁴³ On the contrary, if α_0 is low, regions in the phase diagram may appear where the transition is second order.

The value of α controls the transition to a RL regime. For

$$\alpha > \alpha_{nl} = \frac{3 - 1.76382\epsilon}{3 - 1.03703\epsilon^2} \quad (87)$$

(in this work $\epsilon = 1$ and $\alpha_{nl} = 0.6297\dots$) the transition is toward a RL phase with a 1RSB structure via a RFOT typical of glassy systems. For $\alpha < \alpha_{nl}$ at the lasing

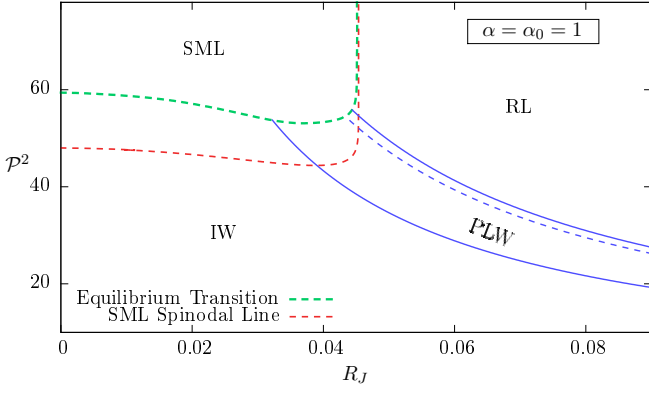


FIG. 11. Phase diagram in the photonics parameters for $a = a_0 = 1$. Dashed red line: spinodal line of the RS SML phase. Dashed green line: thermodynamic transition line. Solid black line: $b_4(q_0 = 0)$ line. Blue lines: transition lines between the $m = 0$ phases. The dashed blue line is the dynamic transition with finite complexity.

threshold the 1RSB phase is unstable, and the transition is toward a RL phase with a FRSB structure. In the latter case the transition is continuous also in the order parameters.

Though we stress here that in any realistic non-linear optical system the 4-body interaction is generally expected to be dominant above the lasing threshold, cf. Sect. I, in cavity-less random lasers and in laser cavities with strong leakages the contribution from linear interactions plays an important role on the stimulated emission and the values of α_0 and α are not expected to be always close to one.

A further important point is that the transition from IW to SML only occurs for a strictly positive value of the coupling coefficient J_0 . This is effectively shown in Fig. 13, where the phase diagrams for $\alpha = \alpha_0 = 1$ and $\alpha = \alpha_0 = 0.7$ are displayed in terms of $R_J^{-1} = J_0/J$ and $\mathcal{P}^2 R_J$. In standard passive mode locking lasers, e.g., the coefficient J_0 accounts for the presence of a saturable absorber in the cavity.³⁸ In cavity-less RL this device, or any analogue one, is obviously not present so that the occurrence of the lasing transition as a mode-locking is not to be given for granted. However, as shown in Fig. 12, starting from a standard laser supporting passive mode-locking and increasing the disorder R_J , we find that the IW/SML mode-locking transition acquires the character of a glassy IW/RL mode-locking transition. This is present even for $J_0 < 0$, as explicitly shown in Fig. 13.

IV. CONCLUSIONS

In this paper we have reported the detailed study of a statistical mechanical model whose degrees of freedom are complex continuous spins satisfying a global spherical constraint and interacting via 2- and 4-body in-

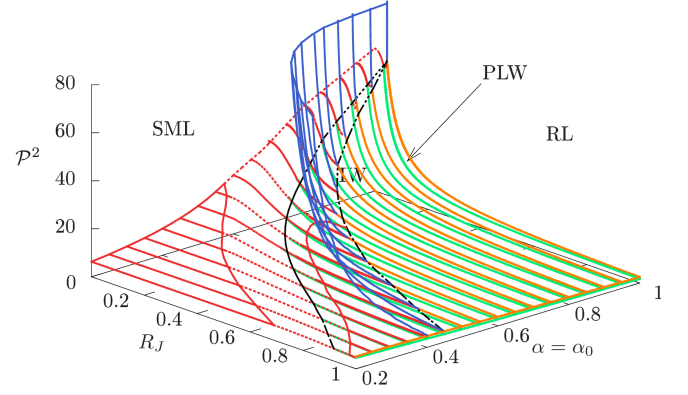


FIG. 12. Phase diagram in the photonics parameters for $\alpha = \alpha_0$ (and $\beta J_0 = 1$). The solid (dashed) red lines correspond to continuous (discontinuous) IW-SML transition. The blue surface is the RL-SML transition, the orange surface the PLW-RL transition and the green surface the IW-PLW transition. The two black lines mark the intersection between the orange-blue and green-red surfaces, respectively.

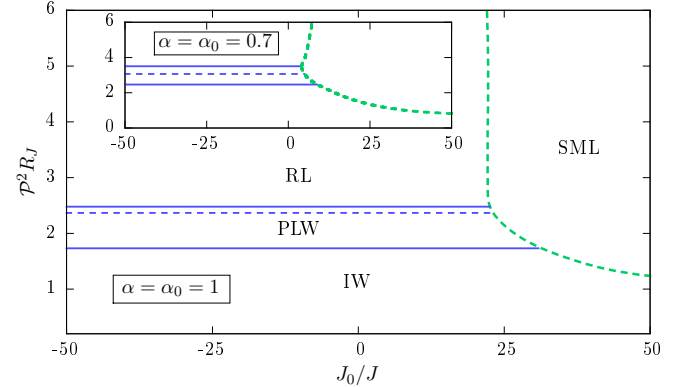


FIG. 13. Phase diagram in the parameters J_0/J vs $\mathcal{P}^2 R_J$ for $\alpha = \alpha_0 = 1$ and $\alpha = \alpha_0 = 0.7$ (inset). The green dashed line corresponds to the equilibrium thermodynamic transition towards the SML phase, the dashed blue line is the dynamic transition between the PLW and RL phases. The continuous blue lines denote thermodynamic IW/PWL and PWL/RL transitions.

teractions. The model gives a statistical description of the complex wave amplitude dynamics in non-linear wave systems. They include, in particular, the multimode laser systems in presence of a non-perturbative degree of randomness and the very interesting limit of random lasers.

We examine in depth the framework of our equilibrium statistical mechanics description of optical systems in stationary, i.e., off-equilibrium, non-linear regimes, among which the paradigmatic laser case, and we discuss the limits of applicability of our theory.

The dynamics of the electromagnetic modes is described by Langevin equations with linear and nonlinear terms whose couplings derive from the spatial overlap of

the modes mediated by the spatial profile of the active medium susceptibility. We have shown that the presence of a continuous spectrum of radiative modes leads to a further contribution to the linear coupling term. We have critically reported how the major difficulty in open and random optically active systems is to express the couplings in the slow amplitude mode basis, i.e., the modes with a *definite* frequency, to which the thermodynamic approach effectively applies.

The primary condition assumed in the model is the absence of dispersion in the Master equation, so that the multimode laser system is Hamiltonian and the steady-state solution of the associated Fokker-Plank equation is given by the Gibbs distribution and the methods of equilibrium statistical mechanics apply. The purely dissipative case corresponds to some well known physical situations, like negligible group velocity dispersion and Kerr effect in standard mode locking lasers and the relevant case of soliton lasers. In the general case the condition is hardly verifiable, though we have shown that in most cases, where the degree of nonlinearity is high enough, there are first order transitions that are expected to be robust by slight modification of the complex coefficients of the dynamics.

We have reported the results for the mean field theory of the model that includes the whole complex mode amplitude dynamics when coupled by both ordered and disordered and linear (2-body) and nonlinear (4-body) interactions. The whole phase diagram obtained via the replica theory has been reported in terms of different sets of external parameters. We adopted, in particular, the description typical of glassy systems undergoing slow relaxation at criticality and dynamic arrest at the transition. In this case the parameters ($\xi_{2,4}$, $b_{2,4}$) are the coefficients of the linear and third order terms in the memory Kernel of a related schematic Mode Coupling Theory^{50,70,73} for the hypothetical dynamics of complex-valued density fluctuations in fluid glass-formers.

Further on, we used an equivalent photonic description in terms of degree of disorder, source pumping rate and degree of non-linearity. Four different optical regimes are found: incoherent fluorescence (IW), standard mode locking (SML), random lasing (RL) and phase locking wave (PLW). In the incoherent wave the modes oscillate independently as in a paramagnet or in a warm liquid. In the standard mode locking the modes are coherent both in phase and in intensity and ultrashort electromagnetic pulses are generated. This ordered regime corresponds to a ferromagnet, or a crystal solid. In the random lasing regime the mode oscillations are frustrated, so the phases are locked but without global ordering and any regular pattern in the intensities. This is a glassy phase, occurring both as a mean-field window glass, for moderately open cavities $\alpha > \alpha_{nl}$ or a spin-glass phase, for very open cavities where linear dumping is not negligible and cannot be treated perturbatively. At last, in the phase locking wave, a novel regime not foreseen in previous statistical mechanical works, phase coherence is

attained, without any intensity coherence (it is an unmagnetized phase). This regime takes place between the incoherent wave and the lasing regimes in presence of a given amount of quenched disorder and it is achievable only when a model includes the dynamics of both phases and intensities.

In this context the random lasing threshold is characterized by the replica symmetry breaking and, at high enough degree of nonlinearity, a whole region with non-vanishing complexity is observed to anticipate the transition. In this sense the light propagating and amplifying in the disordered medium displays glassy behavior. We have shown that this picture is stable against the introduction of a linear coupling and the transition becomes continuous only when the linear coupling is actually dominant. The presence of a small linear coupling, even if not changing the transition, is shown to alter, nevertheless, the structure of the phase diagram non-trivially, so that, e. g., even a transition from standard mode locking to random lasing can be observed increasing the pumping at fixed degree of disorder.

The inclusion of the full complex amplitudes of the modes as fundamental degrees of freedom, rather than the mere mode phases as in previous works^{13,20,21} may be prominent for an experimental test and, in particular, to observe the replica symmetry breaking predicted by the theory.^{9,22} Indeed, the measure of the phase-phase correlations required for measuring the theoretical overlap among the modes is not generally available in the experiments, as the random lasing emission is hardly intense enough to use second-harmonic generation techniques, but intensity correlations can be easily measured.

There are few possible extensions of the previous mean field model considered in this paper. To name some, one could consider the inclusion of correlations in the quenched disordered interactions, further orders of nonlinear interaction, fluctuations of the spherical constraint. Nevertheless, none of these extensions is expected to change the general mean-field picture described in this work, in particular the kind of phases and the nature of the transitions involved.

A more relevant generalization of this approach is the extension to random laser models beyond the mean-field theory, where new features may arise and a more direct comparison with experimental setups is possible, e. g., by generalizing the numerical approach of Refs. [62 and 74] for the pulsed ultrashort mode-locked lasing in ordered statistical mechanical mode networks to the case of quenched disordered interactions and random lasing.

Different approaches are, instead, needed to study the evolution of the system in the general case with a non-negligible presence of dispersion, to discuss the robustness of the picture presented in this paper. The direct analysis of the stochastic dynamics of a finite number of modes is necessary to this aim. Moreover, in this case also the approach to the stationary state would be accessible, providing an appealing integration of the results presented here.

ACKNOWLEDGMENTS

The research leading to these results has received funding from the People Programme (Marie Curie Actions) of the European Union's Seventh Framework Programme FP7/2007-2013/ under REA grant agreement no. 290038, NETADIS project, from the European Research Council through ERC grant agreement no. 247328 - CriPheRaSy project - and from the Italian MIUR under the Basic Research Investigation Fund FIRB2008 program, grant No. RBFR08M3P4, and under the PRIN2010 program, grant code 2010HXAW77-008.

Appendix A: Functional $G[Q, R, m_\sigma, m_\tau]$, Eq. (46).

In this appendix we give the mains steps to derive the functional (46). The procedure follows the standard derivation for spherical model, see e.g. Refs. [16], [73]. Performing the average in Eq. (40) over the random couplings of the Hamiltonian (44) with the Gaussian probability distribution (31), leads to

$$\begin{aligned} \overline{Z^n} &= \int \prod_{j=N}^n \prod_{a=1}^n d\sigma_j^a d\tau_j^a \\ &\times \exp \left\{ \frac{2b_2}{N} [(\sigma^a)^2 + (\tau^a)^2] \right. \\ &\quad \left. + \frac{4b_4}{N^3} [(\sigma^a)^4 + (\tau^a)^4 + 2(\sigma^a)^2 (\tau^a)^2] \right\} \\ &\times \prod_{a,b=1}^n \exp \left\{ \frac{\xi_2}{N} [(\sigma^a \sigma^b)^2 + 2(\sigma^a \tau^b)^2 + (\tau^a \tau^b)^2] \right. \\ &\quad \left. + \frac{3\xi_4}{2N^3} (F^a F^b)^4 \right\}, \end{aligned} \quad (A1)$$

where

$$\begin{aligned} (F^a F^b)^4 &\equiv (\sigma^a \sigma^b)^4 + (\tau^a \tau^b)^4 + 2(\sigma^a \tau^b)^4 \\ &\quad + 4(\sigma^a \sigma^b)^2 (\sigma^a \tau^b)^2 + 4(\tau^a \sigma^b)^2 (\tau^a \tau^b)^2 \\ &\quad + \frac{2}{3} [(\sigma^a \sigma^b)^2 (\tau^a \tau^b)^2 + (\sigma^a \tau^b)^2 (\tau^a \sigma^b)^2 \\ &\quad + 4(\sigma^a \sigma^b)(\sigma^a \tau^b)(\tau^a \sigma^b)(\tau^a \tau^b)], \end{aligned}$$

and we have used the shorthand notation

$$(\sigma^{a_1} \dots \sigma^{a_i})^p \equiv \left(\sum_{j=1}^N \sigma_j^{a_1} \dots \sigma_j^{a_i} \right)^p. \quad (A2)$$

The parameters are those defined in Eqs. (36).

The above expression can be simplified by introducing the matrices Q_{ab} , R_{ab} defined in eqs. (49)-(50), the magnetizations $m_{\sigma;a}$, $m_{\tau;a}$ defined in eq. (51), we have added a replica index to m_σ and m_τ for simplicity of computation, and the additional matrix

$$T_{ab} = \frac{1}{\mathcal{E}} \sum_{j=1}^N \text{Im} [a_j^a a_j^b] = \frac{2}{N} \sum_{j=1}^N \sigma_j^a \tau_j^b. \quad (A3)$$

This is easily achieved by using the Dirac delta function and the identity

$$\int_{-\infty}^{+\infty} dx \delta(x-y) = 1,$$

to impose the definitions as, e.g.,

$$\int_{-\infty}^{\infty} dQ_{ab} \delta[Q_{ab} - [(\sigma^a \sigma^b) + (\tau^a \tau^b)]/N] = 1,$$

and similarly for the others.

Using finally the integral representation

$$\delta(x-y) = \int_{-i\infty}^{i\infty} \frac{d\hat{x}}{2\pi i} e^{-\hat{x}(x-y)}$$

for the delta function, Eq. (A1) can be written as

$$\overline{Z^n} = \int \mathcal{D}\hat{\Phi} \mathcal{D}\Phi e^{-NG[\hat{\Phi}, \Phi]}, \quad (A4)$$

where $\Phi = (Q, R, T, \mathbf{m})$, $\mathbf{m}^a = (m_{\sigma;a}, m_{\tau;a})$, with $\hat{\Phi}$, $\hat{\mathbf{m}}$ the corresponding hatted quantities, and the measure is:

$$\begin{aligned} \mathcal{D}\hat{\Phi} \mathcal{D}\Phi &\equiv \mathcal{N} \prod_{a < b} dQ_{ab} dR_{ab} \prod_{a \leq b} d\hat{Q}_{aa} d\hat{R}_{aa} \\ &\times \prod_{a,b} dT_{ab} d\hat{T}_{ab} \\ &\times \prod_a dm_{\sigma;a} d\hat{m}_{\sigma;a} \prod_a dm_{\tau;a} d\hat{m}_{\tau;a}, \end{aligned}$$

where \mathcal{N} is an unimportant normalization factor. The functional in the exponent reads

$$\begin{aligned} -G[\hat{\Phi}, \Phi] &= \frac{\xi_2}{2} \sum_{ab} [Q_{ab}^2 + R_{ab}^2 + T_{ab}^2] \\ &\quad + \frac{\xi_4}{4} \sum_{ab} [Q_{ab}^4 + R_{ab}^4 + 4Q_{ab}^2 R_{ab}^2 \\ &\quad + \frac{3}{4} T_{ab}^4 + 3T_{ab}^2 (Q_{ab}^2 + R_{ab}^2) \\ &\quad + \frac{1}{4} T_{ab}^2 T_{ba}^2 + T_{ab} T_{ba} (Q_{ab}^2 - R_{ab}^2)] \\ &\quad + \sum_a k(m_{\sigma;a}, m_{\tau;a}) \\ &\quad - \frac{1}{2} \sum_{ab} [\hat{Q}_{ab} Q_{ab} + \hat{R}_{ab} R_{ab} + \hat{T}_{ab} T_{ab}] \\ &\quad - \frac{1}{\sqrt{2}} \sum_a \hat{\mathbf{m}}^a \cdot \mathbf{m}^a + \ln Z[\hat{\Phi}], \end{aligned}$$

where $k(x, y)$ is given in Eq. (48), the 'dot' denotes standard scalar product, and

$$\begin{aligned} Z[\hat{\Phi}] &= \int \prod_{a=1}^n d\sigma_a d\tau_a \\ &\times \exp \left[\frac{1}{2} (\sigma \hat{A} \sigma + \tau \hat{B} \tau + 2\sigma \hat{T} \tau) - \hat{m}_\sigma \sigma - \hat{m}_\tau \tau \right], \end{aligned} \quad (A5)$$

with summation over replica indexes assumed, and $\hat{A}_{ab} = \hat{Q}_{ab} + \hat{R}_{ab}$ while $\hat{B}_{ab} = \hat{Q}_{ab} - \hat{R}_{ab}$. Note that as usual an extra factor 2 is added when needed to the diagonal elements of matrices to account for the extra 1/2 factor coming from the symmetry of the matrix.

In the thermodynamic limit $N \rightarrow \infty$ the integrals in (A4) are dominated by the largest value of the exponent and hence they can be evaluated using the saddle point method. Note that the order of the $N \rightarrow \infty$ and $n \rightarrow 0$ limits is exchanged.

Stationarity of $G[\hat{\Phi}, \Phi]$ with respect to variations of T and \hat{T} leads respectively to the saddle point equations

$$\xi_2 T_{ab} + \frac{\xi_4}{4} [3T_{ab}^3 + 6T_{ab}(Q_{ab}^2 + R_{ab}^2) + T_{ab}T_{ba}^2 + 2T_{ba}(Q_{ab}^2 - R_{ab}^2)] = \frac{1}{2}\hat{T}_{ab}, \quad (\text{A6})$$

$$T_{ab} = 2\langle\sigma^a\tau^b\rangle, \quad (\text{A7})$$

where the average is performed with the probability measure defined in (A5). The original Hamiltonian (30) is invariant under a global phase rotation $a \rightarrow a e^{i\varphi}$, and hence T_{ab} must be symmetric. Thus the only possible solution to (A7) is $T_{ab} = 2\langle\sigma^a\rangle\langle\tau^b\rangle = 2m_\sigma m_\tau$ because without an explicit breaking of the replica equivalence, vectorial RSB, all replicas are identical and single replica quantities cannot depend on the replica. This in turns implies that also \hat{T}_{ab} cannot depend on a and b . The only possible solution to (A6) with replica independent \hat{T}_{ab} and T_{ab} is $\hat{T}_{ab} = T_{ab} = 0$. Then m_σ and m_τ cannot be different from zero simultaneously.

The other consequence of $\hat{T}_{ab} = T_{ab} = 0$ is that integral over σ and τ in (A5) decouples and hence $G[\hat{\Phi}, \Phi]$ for the solution $\hat{T}_{ab} = T_{ab} = 0$ can be written as

$$\begin{aligned} -G[\hat{\Phi}, \Phi] &= F[Q, R, \mathbf{m}] - \frac{1}{4}[\hat{A}A + \hat{B}B] \\ &\quad - \frac{1}{\sqrt{2}}\hat{\mathbf{m}} \cdot \mathbf{m} + W_0[\hat{m}_\sigma, \hat{A}] + W_0[\hat{m}_\tau, \hat{B}]. \end{aligned} \quad (\text{A8})$$

where again the sum over replicas indexes is assumed,

$$F[Q, R, \mathbf{m}] = \frac{1}{2} \sum_{ab} g(Q_{ab}, R_{a,b}) + \sum_a k(m_{\sigma;a}, m_{\tau;a}), \quad (\text{A9})$$

with $g(x, y)$ given in (47), and $W_0[J, K]$ is the massless limit $\Delta \rightarrow 0$ of the connected generating functional of the gaussian theory

$$W_\Delta[J, K] = \ln \int d\sigma \exp\left[-\frac{1}{2}\sigma\Delta\sigma + \frac{1}{2}\sigma K\sigma + J\sigma\right]. \quad (\text{A10})$$

The transformation $(Q, R) \rightarrow (A, B)$ is orthogonal and hence the form $\hat{Q}Q + \hat{R}R$ is invariant, but gain an additional 1/2 factor. Even if m_σ and m_τ cannot be simultaneously non null, we keep both to treat the two cases at the same time. Also we maintain their replica index when needed to simplify the notation.

Stationarity with respect to \hat{Q} and \hat{R} is equivalent to stationarity with respect to \hat{A} and \hat{B} . The stationarity of G with respect to \hat{m}_σ and \hat{A} leads to the saddle point equations

$$\frac{\partial}{\partial \hat{m}_\sigma} W_0[\hat{m}_\sigma, \hat{A}] = \frac{1}{\sqrt{2}} m_\sigma, \quad (\text{A11})$$

$$\frac{\partial}{\partial \hat{A}} W_0[\hat{m}_\sigma, \hat{A}] = \frac{1}{4} A, \quad (\text{A12})$$

from which one recognizes in (A8) the double Legendre transform of $W_0[\hat{m}_\sigma, \hat{A}]$.

The double Legendre transform $\Gamma_\Delta[G, \varphi]$ of $W_\Delta[J, K]$ is defined as

$$\begin{aligned} \Gamma_\Delta[G, \varphi] + W_\Delta[J, K] &= J\varphi + \frac{1}{2}\varphi K\varphi + \frac{1}{2}GK, \\ \frac{\partial}{\partial J} W_\Delta[J, K] &= \varphi, \\ \frac{\partial}{\partial K} W_\Delta[J, K] &= \frac{1}{2}[G + \varphi\varphi]. \end{aligned} \quad (\text{A13})$$

Then comparison with (A8) shows that

$$-W_0[\hat{m}_\sigma, \hat{A}] + \frac{1}{4}\hat{A}A + \frac{1}{\sqrt{2}}\hat{m}_\sigma m_\sigma = \Gamma_0[G, \varphi], \quad (\text{A14})$$

with

$$\varphi = \frac{1}{\sqrt{2}} m_\sigma, \quad \frac{1}{2}A = G + \varphi\varphi. \quad (\text{A15})$$

The double Legendre transform $\Gamma_\Delta[G, \varphi]$ for the Gaussian (free) theory is equal to,⁷⁵⁻⁷⁷

$$\Gamma_\Delta[G, \varphi] = \frac{1}{2}\varphi\Delta\varphi + \frac{1}{2}\Delta G + \frac{1}{2}\text{Tr} \ln G^{-1}, \quad (\text{A16})$$

and can be derived from general arguments or by evaluating it directly. Then, neglecting unnecessary constants,

$$\begin{aligned} -W_0[\hat{m}_\sigma, \hat{A}] + \frac{1}{4}\hat{A}A + \frac{1}{\sqrt{2}}\hat{m}_\sigma m_\sigma &= \\ &= -\frac{1}{2}\text{Tr} \ln[A - m_\sigma \otimes m_\sigma] \\ &= -\frac{1}{2}\text{Tr} \ln A + \frac{1}{2}m_\sigma A^{-1}m_\sigma + O(n^2). \end{aligned} \quad (\text{A17})$$

Stationarity of G with respect to \hat{m}_τ and \hat{B} leads to a similar result. Then collecting all terms

$$\begin{aligned} -G[Q, R, m_\sigma, m_\tau] &= \frac{1}{2} \sum_{a,b} g(Q_{ab}, R_{ab}) \\ &\quad + n k(m_\sigma, m_\tau) \\ &\quad + \frac{1}{2}\text{Tr} \ln A - \frac{m_\sigma^2}{2} \sum_{a,b} (A^{-1})_{ab} \\ &\quad + \frac{1}{2}\text{Tr} \ln B - \frac{m_\tau^2}{2} \sum_{a,b} (B^{-1})_{ab}, \end{aligned} \quad (\text{A18})$$

which completes the derivation of (46):

Appendix B: Solutions of the stationary equations

The equations for the order parameters Q_{ab} , R_{ab} and magnetizations m_σ , m_τ follow from stationarity of the functional $G[Q, R, m_\sigma, m_\tau]$.

Introducing the function $\Lambda(x, y)$, defined in (68), and noticing that $(\partial/\partial y)g(x, y) = \Lambda(y, x)$ because of the symmetry $g(y, x) = g(x, y)$, stationarity with respect to variations of Q_{ab} and R_{ab} with $a \neq b$ leads to the saddle point equation:

$$\Lambda(Q_{ab}, R_{ab}) + (A^{-1})_{ab} + m_\sigma^2 \left[\sum_b (A^{-1})_{ab} \right]^2 + (B^{-1})_{ab} + m_\tau^2 \left[\sum_b (B^{-1})_{ab} \right]^2 = 0, \quad (\text{B1})$$

$$\Lambda(R_{ab}, Q_{ab}) + (A^{-1})_{ab} + m_\sigma^2 \left[\sum_b (A^{-1})_{ab} \right]^2 - (B^{-1})_{ab} - m_\tau^2 \left[\sum_b (B^{-1})_{ab} \right]^2 = 0. \quad (\text{B2})$$

To obtain these equations we have used the property that the sum off all elements of a row (column) of overlap matrices does not depend on the row (column) index.

The function $g(x, y)$ is even in x and y , see (47), then $\Lambda(-x, y) = -\Lambda(x, y)$ while $\Lambda(x, -y) = \Lambda(x, y)$. Consequence of this, if $m_\tau = 0$ then the solution to (B1)-(B2) is $R_{ab} = Q_{ab}$ for $a \neq b$. Vice versa, if $m_\sigma = 0$ then the solution is $R_{ab} = -Q_{ab}$ for $a \neq b$. If $m_\sigma = m_\tau = 0$ then both solutions exist, and are degenerate. Note that $R_{ab} = Q_{ab}$ implies $\langle \tau^a \tau^b \rangle = 0$ while $R_{ab} = -Q_{ab}$ that $\langle \sigma^a \sigma^b \rangle = 0$.

For what concerns the diagonal elements Q_{aa} they are all equal to 1 because of the spherical constraint (43). Similarly $R_{aa} = \bar{R}$ for all a with \bar{R} determined by stationarity via (B2) evaluated for $a = b$.

The analysis of stationarity of $G[Q, R, m_\sigma, m_\tau]$ with respect to variations of m_σ or m_τ simplifies if the solution is specified. The general treatment does not add anything more. Consider the solution with $m_\tau = 0$, the case $m_\sigma = 0$ is similar. Then stationarity leads to the saddle point equation:

$$n \frac{\partial}{\partial m_\sigma} k(m_\sigma, 0) - m_\sigma \sum_{ab} (A^{-1})_{ab} = 0, \quad (\text{B3})$$

which, making use of the identity

$$\frac{1}{n} \sum_{ab} A_{ab} = \frac{1}{\frac{1}{n} \sum_{ab} (A^{-1})_{ab}} \quad (\text{B4})$$

gives

$$m_\sigma = \left[\frac{1}{n} \sum_{ab} A_{ab} \right] \frac{\partial}{\partial m_\sigma} k(m_\sigma, 0). \quad (\text{B5})$$

Inserting this form into (A18), the functional G can be written in the equivalent form

$$\begin{aligned} -G[Q, R, m_\sigma, 0] &= \frac{1}{2} \sum_{a,b} g(Q_{ab}, R_{ab}) \\ &+ \frac{1}{2} \text{Tr} \ln A - \frac{b^2}{2} \sum_{a,b} A_{ab} \\ &+ \frac{1}{2} \text{Tr} \ln B + n k(m_\sigma, 0) \end{aligned} \quad (\text{B6})$$

where $b = (\partial/\partial m_\sigma)k(m_\sigma, 0)$. This form, besides the last term, is the same one would get for a model described by the Hamiltonian (44), but random couplings with $J_0^{(p)} = 0$, and a uniform external field $\sqrt{2}b/\beta$ coupled with the σ_j .³⁷ The factor $\sqrt{2}$ follows from the definition (51) of m_σ and ensures that

$$m_\sigma = \frac{b}{n} \sum_{ab} A_{ab}, \quad (\text{B7})$$

so that (B5) is satisfied.

For overlap matrices with the Parisi replica symmetry breaking scheme¹⁴ the equations can be written more explicitly in terms of their Replica Fourier Transform,⁵⁹⁻⁶¹ defined for a generic matrix M_{ab} in eqs. (56).

The functional $G[Q, R, m_\sigma, m_\tau]$ then takes the form (55), see eg. [37], while the saddle point equations (B1) becomes, as $p_0 = n \rightarrow 0$:

$$\Lambda(Q_0, R_0) - \frac{A_0 - m_\sigma^2}{(A_1)^2} - \frac{B_0 - m_\tau^2}{(B_1)^2} = 0, \quad (\text{B8})$$

and

$$\begin{aligned} \Lambda(Q_r, R_r) - \Lambda(Q_{r-1}, R_{r-1}) \\ - \frac{A_r - A_{r-1}}{A_{\hat{r}} A_{\widehat{r+1}}} - \frac{B_r - B_{r-1}}{B_{\hat{r}} B_{\widehat{r+1}}} = 0, \end{aligned} \quad (\text{B9})$$

for $r = 1, \dots, \mathcal{R}$. Similarly (B2) reads:

$$\Lambda(R_0, Q_0) - \frac{A_0 - m_\sigma^2}{(A_1)^2} + \frac{B_0 - m_\tau^2}{(B_1)^2} = 0, \quad (\text{B10})$$

and, for $r = 1, \dots, \mathcal{R} + 1$,

$$\begin{aligned} \Lambda(R_r, Q_r) - \Lambda(R_{r-1}, Q_{r-1}) \\ - \frac{A_r - A_{r-1}}{A_{\hat{r}} A_{\widehat{r+1}}} + \frac{B_r - B_{r-1}}{B_{\hat{r}} B_{\widehat{r+1}}} = 0, \end{aligned} \quad (\text{B11})$$

with the boundary value $Q_{\mathcal{R}+1} = 1$ and $R_{\mathcal{R}+1} = \bar{R}$. Finally for the case $m_\tau = 0$ (B5), or equivalently (B7), simply becomes

$$m_\sigma = b A_1. \quad (\text{B12})$$

The parameters p_r , except for $p_0 = n$ and $p_{\mathcal{R}+1} = 1$ are not determined. If we require that G be stationary

with respect also to variations of p_r , then we have the additional set of equations

$$\begin{aligned}
g(Q_r, R_r) - g(Q_{r-1}, R_{r-1}) = & \\
\frac{1}{p_r^2} \log \frac{A_{\widehat{r}}}{A_{\widehat{r+1}}} - \frac{A_r - A_{r-1}}{p_r A_{\widehat{r}}} & \\
+ (A_r - A_{r-1}) \left[\sum_{t=1}^{r-1} \frac{A_t - A_{t-1}}{A_{\widehat{t}} A_{\widehat{t+1}}} + \frac{A_0 - m_\sigma^2}{(A_1)^2} \right] & \\
+ \frac{1}{p_r^2} \log \frac{B_{\widehat{r}}}{B_{\widehat{r+1}}} - \frac{B_r - B_{r-1}}{p_r B_{\widehat{r}}} & \\
+ (B_r - B_{r-1}) \left[\sum_{t=1}^{r-1} \frac{B_t - B_{t-1}}{B_{\widehat{t}} B_{\widehat{t+1}}} + \frac{B_0 - m_\tau^2}{(B_1)^2} \right] = 0, & \\
r = 1, \dots, \mathcal{R}. &
\end{aligned}$$

for $r = 1, \dots, \mathcal{R}$ which leads to the *static* solution. The other case of interest, called the *dynamical* solution, is the request that the state be *marginally stable*, that is that the relevant eigenvalue of fluctuations about the stationary point vanishes. For example, this request the 1RSB solution leads to the additional equation (75). See also Appendix C.

Appendix C: Saddle Point Stability Analysis

The evaluation of the integrals in (A4) by the saddle point method requires that at the stationary point the functional $G[\widehat{\Phi}, \Phi]$ attains its minimum value. Convexity of the Legendre transform ensures that $G[Q, R, m_\sigma, m_\tau]$ should also be minimum at the saddle point. However as $n < 1$ the space dimension of Q_{ab} and R_{ab} with $a \neq b$ becomes negative turning the minimum into a maximum. Thus as $n \rightarrow 0$ the functional $G[Q, R, m_\sigma, m_\tau]$ evaluated at the saddle point gives the maximum value with respect to variations of Q and R and the minimum value for variations in m .

The second observation is that $(\delta Q, \delta R)$ and δm fluctuations can be studied separately. Cross-correlations $\delta Q \delta m$ and $\delta R \delta m$ originate only from the $m_\sigma^2 \sum A^{-1}$, or $m_\tau^2 \sum B^{-1}$, term, see (A18). The quadratic form $\delta^2 G$ controlling the fluctuations about the saddle point can then be studied separately in the two orthogonal spaces $(\delta Q, \delta R, 0)$ and $(0, 0, \delta m)$. Stated differently, this means that m fluctuations can be studied for fixed (Q, R) and m fluctuations for fixed (Q, R) .

The stability analysis of m fluctuations it is not dissimilar to that of an ordinary mean-field ferromagnet. Fixing Q and R , from (A18), and using (B3), the m_σ fluctuations in the $m_\tau = 0$ solution are stable if

$$\begin{aligned}
-\frac{\partial^2}{\partial m_\sigma^2} k(m_\sigma, 0) + \frac{1}{n} \sum_{ab} (A^{-1})_{ab} = & \\
= \left[-\frac{\partial^2}{\partial m_\sigma^2} + \frac{1}{m} \frac{\partial}{\partial m_\sigma} \right] k(m_\sigma, 0) \geq 0. & \quad (C1)
\end{aligned}$$

For the model discussed in main text this condition becomes, see (48),

$$8b_4 m_\sigma^2 \geq 0, \quad (C2)$$

and hence for non-negative b_4 the solution $m_\sigma \neq 0$, if it exists, it is always stable.

The analysis of (Q, R) fluctuations is more complex and depends on the RSB structure. To keep the discussion as simple as possible we shall limit ourself to the case $m_\sigma = m_\tau = 0$. The study of the eigenvalues of the Hessian matrix $M^{ab;cd}$ of the (Q, R) fluctuations about the saddle point is unaffected by this choice, however it simplifies the calculations. Moreover, the main consequence of not null m_σ , or m_τ , is a non vanishing Q_0 and R_0 . This modifies the expression of some eigenvalues but not that of the relevant eigenvalues controlling the stability of the saddle point. The number of different eigenvalues, and their expression, depends on the RSB structure. We shall limit ourself to the RS and 1RSB cases only.

The eigenvalues of the Hessian matrix of the (Q, R) fluctuations are solution of the eigenvalue equation

$$\frac{1}{2} \sum_{cd} \left[Q_Q M^{ab;cd} \delta Q^{cd} + Q_R M^{ab;cd} \delta R^{cd} \right] = \Lambda \delta Q^{ab} \quad (C3)$$

$$\frac{1}{2} \sum_{cd} \left[R_Q M^{ab;cd} \delta Q^{cd} + R_R M^{ab;cd} \delta R^{cd} \right] = \Lambda \delta R^{ab} \quad (C4)$$

where

$$\begin{aligned}
Q_Q M^{ab;cd} &= \frac{\partial^2 G}{\partial Q_{ab} \partial Q_{cd}} \\
&= -\Lambda'(Q_{ab}, R_{ab}) \delta_{ab,cd} + {}_+ M^{ab;cd}, & (C5)
\end{aligned}$$

$$\begin{aligned}
Q_R M^{ab;cd} &= \frac{\partial^2 G}{\partial Q_{ab} \partial R_{cd}} \\
&= -\dot{\Lambda}(R_{ab}, Q_{ab}) \delta_{ab,cd} + {}_- M^{ab;cd}, & (C6)
\end{aligned}$$

$$\begin{aligned}
R_R M^{ab;cd} &= \frac{\partial^2 G}{\partial R_{ab} \partial R_{cd}} \\
&= -\Lambda'(R_{ab}, Q_{ab}) \delta_{ab,cd} + {}_+ M^{ab;cd}, & (C7)
\end{aligned}$$

$$\begin{aligned}
R_Q M^{ab;cd} &= \frac{\partial^2 G}{\partial R_{ab} \partial Q_{cd}} \\
&= -\dot{\Lambda}(Q_{ab}, R_{ab}) \delta_{ab,cd} + {}_- M^{ab;cd}, & (C8)
\end{aligned}$$

and

$$\begin{aligned}
{}_+ M^{ab;cd} &= [(A^{-1})_{ac} (A^{-1})_{bd} + (A^{-1})_{ad} (A^{-1})_{bc}] \\
&\quad \pm [(B^{-1})_{ac} (B^{-1})_{bd} + (B^{-1})_{ad} (B^{-1})_{bc}]. & (C9)
\end{aligned}$$

The function $\Lambda(x, y)$ is defined in (68), and we have denoted derivatives with respect to x by a prime and derivatives with respect to y by an overdot. With this notation $\Lambda(x, y) = g'(x, y)$. The factor 1/2 in the eigenvalue equations follows from the symmetry $M^{ab;dc} = M^{ab;cd}$ for $c \neq d$, with the implicit assumption that the diagonal

element $M^{ab;cc}$ is multiplied by 2. The “vectors” δQ^{ab} and δR^{ab} , also symmetric under index exchange, represent the fluctuation of Q and R from the saddle point value. Note that $\delta Q^{aa} = 0$ because its value $Q_{aa} = 1$ is fixed by the spherical constraint (43), and not from stationarity, and cannot fluctuate.

The eigenvalue equations (C3)-(C4) can be solved easily for the RS solution, especially if $Q_0 = R_0 = 0$. For the 1RSB solution the calculation is still feasible using the decomposition of Ref. [16], but becomes rather cumbersome. The more systematic construction of Ref. [78] becomes also rapidly involved as the number of RSB steps increases. The simplest approach is to solve the eigenvalue equations in the Fourier Replica Space using the Replica Fourier Transform.^{60,61}

In the Replica space the metric is defined by the overlap or (co)-distance $a \cap b = r$ between two replicas. This means that replica a and b belong to the same Parisi box of size p_r but to two distinct boxes of size p_{r+1} . This metric defines an ultrametric geometry and hence the four replicas a, b, c, d of $M^{ab;cd}$ can be found only in two different type of configurations.

When the direct overlaps $a \cap b = r$ and $c \cap d = s$ are different $M^{ab;cd}$ can depend on only one cross-overlap:

$$M^{ab;cd} = M_t^{r,s}, \quad t = \max(a \cap c, a \cap d, b \cap c, b \cap d). \quad (\text{C10})$$

These configurations are called *Longitudinal-Anomalous* (LA). When $r = s$ two types of configurations are possible. The first are the LA configurations with $r = s$. However a second, different type, of configurations appears when the cross-overlap between (a, b) and (c, d) is larger than r . For these configurations $M^{ab;cd}$ depends on two cross-overlaps:

$$M^{ab;cd} = M_{u,v}^{r,r}, \quad \begin{aligned} u &= \max(a \cap c, a \cap d), \\ v &= \max(b \cap c, b \cap d), \end{aligned} \quad (\text{C11})$$

with $u, v \geq r + 1$. These configurations are called *Replicon*.⁷⁹ The Replicon and LA sectors are orthogonal to each other and the eigenvalue equations in the two sectors decoupled thus block diagonalizing the Hessian matrix.

In the Replicon sector the eigenvalue equations in the Fourier Replica Space read:

$$QQM_{\hat{k},\hat{l}}^{r,r} \delta Q_{\hat{k},\hat{l}}^{r,r} + QR M_{\hat{k},\hat{l}}^{r,r} \delta R_{\hat{k},\hat{l}}^{r,r} = \Lambda \delta Q_{\hat{k},\hat{l}}^{r,r}, \quad (\text{C12})$$

$$RRM_{\hat{k},\hat{l}}^{r,r} \delta Q_{\hat{k},\hat{l}}^{r,r} + RR M_{\hat{k},\hat{l}}^{r,r} \delta R_{\hat{k},\hat{l}}^{r,r} = \Lambda \delta R_{\hat{k},\hat{l}}^{r,r}, \quad (\text{C13})$$

where

$$QQM_{\hat{k},\hat{l}}^{r,r} = -\Lambda'(Q_r, R_r) + \frac{1}{A_{\hat{k}} A_{\hat{l}}} + \frac{1}{B_{\hat{k}} B_{\hat{l}}} \quad (\text{C14})$$

$$RRM_{\hat{k},\hat{l}}^{r,r} = -\Lambda'(R_r, Q_r) + \frac{1}{A_{\hat{k}} A_{\hat{l}}} + \frac{1}{B_{\hat{k}} B_{\hat{l}}} \quad (\text{C15})$$

$$RQM_{\hat{k},\hat{l}}^{r,r} = -\dot{\Lambda}(Q_r, R_r) + \frac{1}{A_{\hat{k}} A_{\hat{l}}} - \frac{1}{B_{\hat{k}} B_{\hat{l}}} \quad (\text{C16})$$

$$QR M_{\hat{k},\hat{l}}^{r,r} = QR M_{\hat{k},\hat{l}}^{r,r}. \quad (\text{C17})$$

For each (r, k, l) , with $r = 0, \dots, \mathcal{R}$ and $k, l = r + 1, \dots, \mathcal{R} + 1$, the Replicon eigenvalues ${}_{1,2}\Lambda(r; k, l)$ are obtained from the eigenvalue of a 2×2 real symmetric matrix, and are hence real. Each eigenvalue has multiplicity:

$$\mu(r; k, l) = \frac{p_0}{2} \bar{\delta}_k \bar{\delta}_l \delta_r(k, l) \quad (\text{C18})$$

where for $k > r + 1$

$$\bar{\delta}_k = \frac{1}{p_k} - \frac{1}{p_{k-1}}, \quad (\text{C19})$$

while $\bar{\delta}_{r+1} = 1/p_{r+1}$ for $k = r + 1$, and

$$\delta_r(k, l) = p_r - (1 + \delta_{k,r+1} + \delta_{l,r+1}) p_{r+1}. \quad (\text{C20})$$

In the LA sector the eigenvalue equations are more complex. The LA eigenvalues $\Lambda(k)$ are labelled by the single index $k = 0, \dots, \mathcal{R} + 1$ and for each k are obtained from the eigenvalues of a $(2\mathcal{R} + 3) \times (2\mathcal{R} + 3)$ matrix.

In the Fourier Replica Space the eigenvalue equations in the LA sector take the form:

$$\sum_{s=0}^{\mathcal{R}+1} \left[[\delta_{r,s} QQ M_{\widehat{r+1},\hat{k}}^{r,r} + \frac{1}{4} \delta_s^{(k-1)} QQ M_{\hat{k}}^{r,s}] \delta Q_{\hat{k}}^s \right. \quad (\text{C21})$$

$$\left. + [\delta_{r,s} QR M_{\widehat{r+1},\hat{k}}^{r,r} + \frac{1}{4} \delta_s^{(k-1)} QR M_{\hat{k}}^{r,s}] \delta R_{\hat{k}}^s \right] = \Lambda \delta Q_{\hat{k}}^r$$

$$\sum_{s=0}^{\mathcal{R}+1} \left[[\delta_{r,s} RQ M_{\widehat{r+1},\hat{k}}^{r,r} + \frac{1}{4} \delta_s^{(k-1)} RQ M_{\hat{k}}^{r,s}] \delta Q_{\hat{k}}^s \right. \quad (\text{C22})$$

$$\left. + [\delta_{r,s} RR M_{\widehat{r+1},\hat{k}}^{r,r} + \frac{1}{4} \delta_s^{(k-1)} RR M_{\hat{k}}^{r,s}] \delta R_{\hat{k}}^s \right] = \Lambda \delta R_{\hat{k}}^r$$

for $r = 0, \dots, \mathcal{R}$ and

$$\sum_{s=0}^{\mathcal{R}+1} \frac{1}{4} \delta_s^{(k-1)} \left[RQ M_{\hat{k}}^{\mathcal{R}+1,s} \delta Q_{\hat{k}}^s + RR M_{\hat{k}}^{\mathcal{R}+1,s} \delta R_{\hat{k}}^s \right] = 2 \Lambda \delta R_{\hat{k}}^{\mathcal{R}+1} \quad (\text{C23})$$

with $\delta Q_{\hat{k}}^{\mathcal{R}+1} = 0$ for $r = \mathcal{R} + 1$, where

$$\delta_s^{(k)} = p_s^{(k)} - p_{s+1}^{(k)}, \quad p_s^{(k)} = \begin{cases} p_s & s \leq k, \\ 2p_s & s > k. \end{cases} \quad (\text{C24})$$

The factor 2 in (C23) follows from the multiplicity of the diagonal terms. The coefficients of these equations are

$$QQ M_{\hat{k}}^{r,s} = A M_{\hat{k}}^{r,s} + B M_{\hat{k}}^{r,s}, \quad (\text{C25})$$

$$RR M_{\hat{k}}^{r,s} = A M_{\hat{k}}^{r,s} + B M_{\hat{k}}^{r,s} \quad (\text{C26})$$

$$- 2\Lambda'(\bar{R}, 1) \delta_{r,s} \delta_{r,\mathcal{R}+1}, \quad (\text{C27})$$

$$QR M_{\hat{k}}^{r,s} = A M_{\hat{k}}^{r,s} - B M_{\hat{k}}^{r,s}, \quad (\text{C28})$$

$$RQ M_{\hat{k}}^{r,s} = QR M_{\hat{k}}^{r,s},$$

where $(C = A, B)$

$$\begin{aligned} {}_C M_{\hat{k}}^{r,s} &= 4 \frac{(C^{-1})_t}{C_{\hat{k}}}, & k > t = \min(r, s), \\ {}_C M_{\hat{k}}^{r,s} &= 2 \sum_{u=k}^t p_u [(C_u^{-1})^2 - (C_{u-1}^{-1})^2] \\ &\quad + 4 \frac{(C^{-1})_t}{C_{t+1}}, & k \leq t = \min(r, s), \end{aligned} \quad (C29)$$

and

$$(C^{-1})_t = \sum_{k=0}^t \frac{1}{p_k} \left[\frac{1}{C_{\hat{k}}} - \frac{1}{C_{\hat{k}+1}} \right]. \quad (C30)$$

Each eigenvalue has multiplicity

$$\mu(k) = p_0 \bar{\delta}_k, \quad (C31)$$

with $\bar{\delta}_k$ defined in (C19) if $k > 0$ and $\bar{\delta}_0 = 1/p_0$ for $k = 0$.

If $Q_0 = R_0 = 0$ then $(A^{-1})_0 = (B^{-1})_0 = 0$ and

$$\forall k : \quad {}_C M_{\hat{k}}^{r,s} = 0, \quad \text{if } \min(r, s) = 0. \quad (C32)$$

The LA eigenvalue equations (C21)-(C22) for $r = 0$ then decouple from the others and read:

$$\begin{aligned} {}_{QQ} M_{1,\hat{k}}^{0,0} \delta Q_{\hat{k}}^0 + {}_{QR} M_{1,\hat{k}}^{0,0} \delta R_{\hat{k}}^0 &= \Lambda \delta Q_{\hat{k}}^0, \\ {}_{RQ} M_{1,\hat{k}}^{0,0} \delta Q_{\hat{k}}^0 + {}_{RR} M_{1,\hat{k}}^{0,0} \delta R_{\hat{k}}^0 &= \Lambda \delta R_{\hat{k}}^0. \end{aligned} \quad (C33)$$

Comparison with (C12)-(C13) readily shows:

$${}_{1,2} \Lambda(k) = {}_{1,2} \Lambda(0; 1, l), \quad l = \max(1, k). \quad (C34)$$

Appendix D: RS Saddle Point Hessian Eigenvalues

For $\mathcal{R} = 0$ and $Q_0 = R_0 = 0$ the only non-null coefficients of the eigenvalues equations are

$${}_{QQ} M_{1,\hat{1}}^{0,0} = -\Lambda'(0, 0) + 2 \frac{1 + \bar{R}^2}{(1 - \bar{R}^2)^2} \quad (D1)$$

$${}_{RR} M_{1,\hat{1}}^{0,0} = -\Lambda'(0, 0) + 2 \frac{1 + \bar{R}^2}{(1 - \bar{R}^2)^2} \quad (D2)$$

$${}_{RQ} M_{1,\hat{1}}^{0,0} = -4 \frac{\bar{R}}{(1 - \bar{R}^2)^2} \quad (D3)$$

$${}_{QR} M_{1,\hat{1}}^{0,0} = {}_{RQ} M_{1,\hat{1}}^{0,0}. \quad (D4)$$

and

$${}_{RR} M_0^{1,1} = {}_{RR} M_{\hat{1}}^{1,1} = -2\Lambda'(\bar{R}, 1) + 4 \frac{1 + \bar{R}^2}{(1 - \bar{R}^2)^2} \quad (D5)$$

Then the eigenvalues in the Replicon sector are:

$${}_1 \Lambda(0; 1, 1) = -\Lambda'(0, 0) + \frac{2}{(1 + \bar{R})^2} \quad (D6)$$

$${}_2 \Lambda(0; 1, 1) = -\Lambda'(0, 0) + \frac{2}{(1 - \bar{R})^2} \quad (D7)$$

each with multiplicity $\mu(0; 1, 1) = p_0(p_0 - 3)/2$. In the LA sector the eigenvalues read:

$${}_1 \Lambda(k) = -\Lambda'(0, 0) + \frac{2}{(1 + \bar{R})^2} \quad (D8)$$

$${}_2 \Lambda(k) = -\Lambda'(0, 0) + \frac{2}{(1 - \bar{R})^2} \quad (D9)$$

$${}_3 \Lambda(k) = -\frac{1}{2} \Lambda'(\bar{R}, 1) + \frac{1 + \bar{R}^2}{(1 - \bar{R}^2)^2} \quad (D10)$$

with the $k = 0$ eigenvalue (Longitudinal) of multiplicity $\mu(0) = 1$ and the $k = 1$ eigenvalues (Anomalous) of multiplicity $\mu(1) = p_0 - 1$.

The relevant eigenvalues for the stability of the RS solution with $\bar{R} \geq 0$ are, cf. (68) for $\Lambda(x, y)$,⁸⁰

$${}_1 \Lambda(0; 1, 1) = -2\xi_2 + \frac{2}{(1 + \bar{R})^2} \quad (D11)$$

$${}_3 \Lambda(0) = -(\xi_2 + 2\xi_4 + 3\xi_4 \bar{R}^2) + \frac{1 + \bar{R}^2}{(1 - \bar{R}^2)^2}. \quad (D12)$$

If $\bar{R} = 0$ the Replicon eigenvalue is positive below the line $\xi_2 = 1$ but the LA eigenvalue is positive only below the line $\xi_2 + 2\xi_4 = 1$. Above this line an the RS phase with $\bar{R} = 0$ (IW phase) is replaced by the RS phase with $\bar{R} \neq 0$ (Phase-Locking Wave phase). The latter remain stable below the critical line

$$\begin{cases} \xi_2 = \frac{1}{(1+t)^2} \\ \xi_4 = \frac{2t}{(2+t^2)(1+t)(1-t^2)} \end{cases} \quad 0 \leq t = |\bar{R}| \leq 1 \quad (D13)$$

where the eigenvalue ${}_1 \Lambda(0; 1, 1)$ vanishes, solid blue line in Figure 1.

Appendix E: 1RSB Saddle Point Hessian Eigenvalues

We discuss only the solution $R_{ab} = Q_{ab}$, the analysis for the solution $R_{ab} = -Q_{ab}$ being similar.

The coefficients of the eigenvalue equation in the Replicon sector are

$${}_{QQ} M_{\hat{k},\hat{l}}^{r,r} = -\Lambda'(Q_r, Q_r) + \frac{1}{A_{\hat{k}} A_{\hat{l}}} + \frac{1}{(B_2)^2} \quad (E1)$$

$${}_{RR} M_{\hat{k},\hat{l}}^{r,r} = {}_{QQ} M_{\hat{k},\hat{l}}^{r,r} \quad (E2)$$

$${}_{RQ} M_{\hat{k},\hat{l}}^{r,r} = -\Lambda'(Q_r, Q_r) + \frac{1}{A_{\hat{k}} A_{\hat{l}}} - \frac{1}{(B_2)^2} \quad (E3)$$

$${}_{QR} M_{\hat{k},\hat{l}}^{r,r} = {}_{RQ} M_{\hat{k},\hat{l}}^{r,r}. \quad (E4)$$

with eigenvalues

$${}_1\Lambda(r; k, l) = -\Lambda'(Q_r, Q_r) - \dot{\Lambda}(Q_r, Q_r) + \frac{2}{A_k A_l}, \quad (\text{E5})$$

$${}_2\Lambda(r; k, l) = -\Lambda'(Q_r, Q_r) + \dot{\Lambda}(Q_r, Q_r) + \frac{2}{(B_2)^2}, \quad (\text{E6})$$

with $r = 0, 1$ and $k, l \geq r+1$. Then for $(r, k, l) = (1, 2, 2)$:

$${}_1\Lambda(1; 2, 2) = -2(\xi_2 + 9\xi_4 Q_1^2) + \frac{2}{(1 + \bar{R} - 2Q_1)^2}, \quad (\text{E7})$$

$${}_2\Lambda(1; 2, 2) = -2(\xi_2 + \xi_4 Q_1^2) + \frac{2}{(1 - \bar{R})^2}. \quad (\text{E8})$$

and multiplicity $\mu(1; 2, 2) = (p_0/2)(p_1 - 3)$. For $(r, k, l) = (0, 2, 2)$:

$${}_1\Lambda(0; 2, 2) = -2\xi_2 + \frac{2}{(1 + \bar{R} - 2Q_1)^2}, \quad (\text{E9})$$

$${}_2\Lambda(0; 2, 2) = -2\xi_2 + \frac{2}{(1 - \bar{R})^2}, \quad (\text{E10})$$

and multiplicity $\mu(0; 2, 2) = (p_0/2)(1 - 1/p_1)^2(p_0 - p_1)$. For $(r, k, l) = (0, 1, 1)$:

$${}_1\Lambda(0; 1, 1) = -2\xi_2 + \frac{2}{[1 + \bar{R} - 2(1 - p_1)Q_1]^2} \quad (\text{E11})$$

$${}_2\Lambda(0; 1, 1) = {}_2\Lambda(0; 2, 2) \quad (\text{E12})$$

and multiplicity $\mu(0; 1, 1) = (p_0/2)(1/p_1^2)(p_0 - 3p_1)$. Finally for $(r, k, l) = (0, 2, 1)$ or $(r, k, l) = (0, 1, 2)$:

$${}_1\Lambda(0; 2, 1) = -2\xi_2 \quad (\text{E13})$$

$$+ \frac{2}{(1 + \bar{R} - 2Q_1)[1 + \bar{R} - 2(1 - p_1)Q_1]} \quad (\text{E14})$$

and ${}_1\Lambda(0; 1, 2) = {}_1\Lambda(0; 2, 1)$. The multiplicity of these each of these eigenvalues is $\mu(0; 2, 1) = \mu(0; 1, 2) = (p_0/2)(1/p_1)(1 - 1/p_1)(p_0 - 2p_1)$. The total dimension of the Replicon sector is then $p_0(p_0 - 5)$.

The calculation of the eigenvalues in the LA sector for $\mathcal{R} = 1$ requires the evaluation for each k of the eigenvalues of a 5×5 matrix. Each eigenvalue has multiplicity respectively: $\mu(0) = 1$, $\mu(1) = p_0/p_1 - 1$ and $\mu(2) = p_0 - p_0/p_1$. The total dimension of the LA sector is then $5p_0$, which added to the dimension of the Replicon sector gives the total dimension p_0^2 of the (Q_{ab}, R_{ab}) space.

For the solution with $Q_0 = R_0 = 0$ the 5×5 matrix is partially diagonal and for each $k = 0, 1, 2$ the first two eigenvalues read, cf. (C34):

$${}_1\Lambda(k) = {}_1\Lambda(0; 1, l), \quad l = \max(1, k). \quad (\text{E15})$$

When $R_{ab} = Q_{ab}$, and $Q_0 = R_0 = 0$, a straightforward calculation shows that if $\min(r, s) = 1$ then

$$\begin{aligned} {}_A M_2^{r,s} &= 4 \frac{A_1^{-1}}{A_2} \\ {}_A M_k^{r,s} &= 4 \frac{A_1^{-1}}{A_2} + 2p_1(A_1^{-1})^2, \quad k = 0, 1. \\ {}_B M_k^{r,s} &= 0 \quad k = 0, 1, 2 \end{aligned} \quad (\text{E16})$$

while

$${}_A M_2^{2,2} = 2 \left[\frac{1}{(A_2)^2} + 2 \frac{A_1^{-1}}{A_2} \right], \quad (\text{E17})$$

$${}_A M_k^{2,2} = 2 \left[\frac{1}{(A_2)^2} + 2 \frac{A_1^{-1}}{A_2} + p_1(A_1^{-1})^2 \right], \quad k = 0, 1 \quad (\text{E18})$$

$${}_B M_k^{2,2} = \frac{2}{(B_2)^2}, \quad k = 0, 1, 2$$

and

$${}_{RR} M_k^{2,2} = {}_A M_k^{2,2} + \frac{2}{(B_2)^2} - 2\Lambda'(\bar{R}, 1). \quad (\text{E19})$$

The remaining three eigenvalues are then obtained from an eigenvalue equation of the form

$$\begin{cases} (a+b)x + (c+b)y + dz = \Lambda x \\ (c+b)x + (a+b)y + dz = \Lambda y \\ \frac{b}{2}x + \frac{b}{2}y + \frac{e}{2}z = \Lambda z \end{cases} \quad (\text{E20})$$

where

$$\begin{aligned} a &= {}_{QQ} M_{2,k}^{1,1} = {}_{RR} M_{2,k}^{1,1} \\ b &= \frac{1}{4} \delta_1^{(k-1)} {}_A M_k^{1,1} = \frac{1}{4} \delta_1^{(k-1)} {}_A M_k^{2,1} \\ c &= {}_{QR} M_{2,k}^{1,1} = {}_{RQ} M_{2,k}^{1,1} \\ d &= \frac{1}{4} \delta_2^{(k-1)} {}_A M_k^{1,2} \\ e &= \frac{1}{4} \delta_2^{(k-1)} {}_{RR} M_k^{2,2}. \end{aligned} \quad (\text{E21})$$

The equation (E20) admits two types of solution. The first for $y = -x$ and $z = 0$ and leads to the eigenvalue $\Lambda = a - c$, i.e.,

$${}_3\Lambda(k) = {}_2\Lambda(1; 2, 2), \quad k = 0, 1, 2. \quad (\text{E22})$$

The other two eigenvalues, for $x = y$ and $z \neq 0$, read instead

$${}_4\Lambda(k) = \frac{1}{2} \left[T + \sqrt{T^2 - 4\Delta} \right] \quad (\text{E23})$$

$${}_5\Lambda(k) = \frac{1}{2} \left[T - \sqrt{T^2 - 4\Delta} \right] \quad (\text{E24})$$

where

$$T = a + 2b + c + \frac{e}{2}, \quad \Delta = \frac{e}{2}(a + 2b + c) - db. \quad (\text{E25})$$

The explicit form of a, b, c, d, e depends on the value of k . For $k = 0, 1$ one has:

$$b = (p_1 - 1) \left[2 \frac{A_1^{-1}}{A_2} + p_1 (A_1^{-1})^2 \right], \quad (\text{E26})$$

$$d = 2 \frac{A_1^{-1}}{A_2} + p_1 (A_1^{-1})^2, \quad (\text{E27})$$

$$e = -\Lambda'(\bar{R}, 1) + \frac{1}{(A_2)^2} + 2 \frac{A_1^{-1}}{A_2} + p_1 (A_1^{-1})^2 + \frac{1}{(B_2)^2}, \quad (\text{E28})$$

and

$$a + 2b + c = -\Lambda'(Q_1, Q_1) - \dot{\Lambda}(Q_1, Q_1) + \frac{2}{(A_2)^2} + 2(p_1 - 1) \left[2 \frac{A_1^{-1}}{A_2} + p_1 (A_1^{-1})^2 \right]. \quad (\text{E29})$$

For $k = 2$ one has instead:

$$b = (p_1 - 2) \frac{A_1^{-1}}{A_2}, \quad (\text{E30})$$

$$d = 2 \frac{A_1^{-1}}{A_2}, \quad (\text{E31})$$

$$e = -\Lambda'(\bar{R}, 1) + \frac{1}{(A_2)^2} + 2 \frac{A_1^{-1}}{A_2} + \frac{1}{(B_2)^2}, \quad (\text{E32})$$

and

$$a + 2b + c = -\Lambda'(Q_1, Q_1) - \dot{\Lambda}(Q_1, Q_1) + \frac{2}{(A_2)^2} + 2(p_1 - 2) \frac{A_1^{-1}}{A_2}. \quad (\text{E33})$$

The eigenvalues $_{4,5}\Lambda(k)$ are always positive or complex, with positive real part in the whole 1RSB phase with $R_1 = Q_1$.

The relevant eigenvalues for the stability of the 1RSB solution are $_{1}\Lambda(1; 2, 2)$, which controls the stability with respect to Q_1 , and $_{1}\Lambda(0; 1, 1)$, which controls the fluctuations with respect to $Q_0 = 0$. The vanishing of $_{1}\Lambda(1; 2, 2)$ leads to the *marginal condition*, while the vanishing of $_{1}\Lambda(0; 1, 1)$ marks the end of the 1RSB phase and the appearance of a 1FRSB phase. Using the saddle point equation, the critical 1RSB-1FRSB line in the limit $p_0 = n \rightarrow 0$ is

$$\begin{cases} \xi_2 = \frac{1}{\bar{a}^2 x^2} (1 - y_0 + x y_0)^2 \\ \xi_4 = \frac{4}{3\bar{a}^2} \frac{(1 - y_0 + x y_0)^4}{x^2 y (1 - y_0)} \end{cases} \quad (\text{E34})$$

where $x = p_1 \in [0, 1]$ and $y_0 = 0.38957 \dots$ is the solution of $z(y_0) = (1 + y_0)/2$ with $z(y)$ defined in (74), solid black line in Figure 1. Note that for $x = 1$

$$_{1}\Lambda(0; 1, 1) = -2\xi_2 + \frac{2}{(1 + \bar{R})^2} \quad (\text{E35})$$

and one recovers the relevant Replicon eigenvalue of the RS solution. As a consequence the RS and 1RSB critical lines meet at the tricritical point. This is a general result.

* luca.leuzzi@cnr.it

- ¹ V. Letokhov, Soviet Journal of Experimental and Theoretical Physics **26**, 835 (1968).
- ² V. M. Markushev, V. F. Zolin, and C. M. Briskina, Soviet Journal of Quantum Electronics **16**, 281 (1986).
- ³ C. Guedard, D. Husson, C. Sauteret, F. Auzel, and A. Migus, JOSA B **10**, 2358 (1993).
- ⁴ D. S. Wiersma and A. Lagendijk, Phys. Rev. E **54**, 4256 (1996).
- ⁵ D. S. Wiersma, Nature physics **4**, 359 (2008).
- ⁶ S. Mujumdar, V. Türeci, R. Torre, and D. S. Wiersma, Phys. Rev. A **76**, 033807 (2007).
- ⁷ D. Anglos, A. Stassinopoulos, R. N. Das, G. Zacharakis, M. Psyllaki, R. Jakubiak, R. A. Vaia, E. P. Giannelis, and S. H. Anastasiadis, J. Opt. Soc. Am. B **21**, 208 (2004).
- ⁸ K. L. van der Molen, A. P. Mosk, and A. Lagendijk, Phys. Rev. A **74**, 053808 (2006).
- ⁹ N. Ghofraniha, I. Viola, F. Di Maria, G. Barbarella, G. Gigli, L. Leuzzi, and C. Conti, Nat. Commun. **6**, 6058 (2014).
- ¹⁰ D. Sharma, H. Ramachandran, and N. Kumar, Opt. Lett. **31**, 1806 (2006).

- ¹¹ S. Lepri, S. Cavalieri, G.-L. Oppo, and D. S. Wiersma, Phys. Rev. A **75**, 063820 (2007).
- ¹² M. P. A. Fisher, P. B. Weichman, G. Grinstein, and D. S. Fisher, Phys. Rev. B **40**, 546 (1989).
- ¹³ L. Angelani, C. Conti, G. Ruocco, and F. Zamponi, Phys. Rev. Lett. **96**, 065702 (2006).
- ¹⁴ M. Mézard, G. Parisi, and M. A. Virasoro, *Spin glass theory and beyond* (World Scientific, Singapore, 1987).
- ¹⁵ T.R. Kirkpatrick and D. Thirumalai, Phys. Rev. Lett. **58**, 2091 (1987).
- ¹⁶ A. Crisanti and H.-J. Sommers, Z. Phys. B **92**, 341 (1992).
- ¹⁷ W. Götze and L. Sjögren, Reports on Progress in Physics **55**, 241 (1992).
- ¹⁸ L. Leuzzi and T. M. Nieuwenhuizen, *Thermodynamics of the Glassy State* (CRC Press, Taylor & Francis Group, 2007).
- ¹⁹ L. Angelani, C. Conti, G. Ruocco, and F. Zamponi, Phys. Rev. B **74**, 104207 (2006).
- ²⁰ L. Leuzzi, C. Conti, V. Folli, L. Angelani, and G. Ruocco, Phys. Rev. Lett. **102**, 083901 (2009).
- ²¹ C. Conti and L. Leuzzi, Phys. Rev. B **83**, 134204 (2011).
- ²² F. Antenucci, A. Crisanti, and L. Leuzzi, (2014),

- arXiv:1412.8748.
- ²³ F. Antenucci, C. Conti, A. Crisanti, and L. Leuzzi, Phys. Rev. Lett. **114**, 043901 (2015).
 - ²⁴ G. Hackenbroich, J. Phys. A **38**, 10537 (2005).
 - ²⁵ O. Zeitsev and L. Deych, Phys. Rev. A **81**, 023822 (2010).
 - ²⁶ I. Rotter, Journal of Physics A: Mathematical and Theoretical **42**, 153001 (2009).
 - ²⁷ A. Fox and T. Li, Quantum Electronics, IEEE Journal of **4**, 460 (1968).
 - ²⁸ S. M. Dutra and G. Nienhuis, Phys. Rev. A **62**, 063805 (2000).
 - ²⁹ H. E. Türeci, A. D. Stone, and B. Collier, Phys. Rev. A **74**, 043822 (2006).
 - ³⁰ O. Zeitsev and L. Deych, Journal of Optics **12**, 024001 (2010).
 - ³¹ C. Viviescas and G. Hackenbroich, Phys. Rev. A **67**, 013805 (2003).
 - ³² H. Feshbach, Annals of Physics **19**, 287 (1962).
 - ³³ G. Hackenbroich, C. Viviescas, and F. Haake, Phys. Rev. Lett. **89**, 083902 (2002).
 - ³⁴ C. Viviescas and G. Hackenbroich, J. Opt. B: Quantum and Semiclassical Optics **6**, 211 (2004).
 - ³⁵ E. Jaynes and F. W. Cummings, Proceedings of the IEEE **51**, 89 (1963).
 - ³⁶ B. W. Shore and P. L. Knight, J. Mod. Opt. **40**, 1195 (1993).
 - ³⁷ A. Crisanti and L. Leuzzi, Nuclear Physics B **870**, 176 (2013).
 - ³⁸ H. Haus, Selected Topics in Quantum Electronics, IEEE Journal of **6**, 1173 (2000).
 - ³⁹ H. E. Türeci, L. Ge, S. Rotter, and A. D. Stone, Science **320**, 643 (2008).
 - ⁴⁰ H. E. Türeci, A. D. Stone, L. Ge, S. Rotter, and R. J. Tandy, Nonlinearity **22**, C1 (2009).
 - ⁴¹ S. Esterhazy, D. Liu, M. Liertz, A. Cerjan, L. Ge, K. G. Makris, A. D. Stone, J. M. Melenk, S. G. Johnson, and S. Rotter, Phys. Rev. A **90**, 023816 (2014).
 - ⁴² T. R. Kirkpatrick, D. Thirumalai, and P. G. Wolynes, Phys. Rev. A **40**, 1045 (1989).
 - ⁴³ A. Gordon and B. Fischer, Phys. Rev. Lett. **89**, 103901 (2002).
 - ⁴⁴ C.-J. Chen, P. K. A. Wai, and C. R. Menyuk, Opt. Lett. **19**, 198 (1994).
 - ⁴⁵ O. Gat, A. Gordon, and B. Fischer, Phys. Rev. E **70**, 046108 (2004).
 - ⁴⁶ A. Gordon and B. Fischer, Optics Communications **223**, 151 (2003).
 - ⁴⁷ It is said spherical using the naming adopted in spin systems⁸¹ where spins σ_i are approximated by continuous real fields taking values on the N -dimensional hypersphere $\sum_{i=1}^N \sigma_i^2$. Here, in the photonic amplitude model, unlike the classic spherical spin model, the global spherical constraint is formally in the \mathbb{C}^N space of N complex degrees of freedom.
 - ⁴⁸ D. S. Wiersma and S. Cavalieri, Nature **414**, 708 (2001), 10.1038/414708a.
 - ⁴⁹ T. Nakamura, T. Takahashi, and S. Adachi, Phys. Rev. B **81**, 125324 (2010).
 - ⁵⁰ W. Götze, *Complex Dynamics of Glass-Forming Liquids: A Mode-Coupling Theory* (Oxford University Press, 2009).
 - ⁵¹ S. F. Edwards and P. W. Anderson, Journal of Physics F: Metal Physics **5**, 965 (1975).
 - ⁵² G. Parisi, Phys. Rev. Lett. **43**, 1754 (1979).
 - ⁵³ G. Parisi, J. Phys. A **13**, L115 (1980).
 - ⁵⁴ F. Guerra, Comm. Math. Phys. **233**, 1 (2003).
 - ⁵⁵ M. Talagrand, Ann. Math. **163**, 221 (2006).
 - ⁵⁶ M. Mézard, G. Parisi, N. Sourlas, G. Toulouse, and M. Virasoro, Phys. Rev. Lett. **52**, 1156 (1984).
 - ⁵⁷ The $\sqrt{2}$ is chosen to have real and imaginary parts of the magnetization ranging from -1 to 1 in the case of total energy equipartition among modes, i.e., $|a_j| = 1$, for all j , and between real and imaginary part, i.e., $\sigma^2 = \tau^2$.
 - ⁵⁸ We use the symbol \mathcal{R} instead of the usual R for number of RSB to avoid possible confusion with the matrix R_{ab} .
 - ⁵⁹ Marc Mézard and Giorgio Parisi, J. Phys. I France **1**, 809 (1991).
 - ⁶⁰ C. De Dominicis, D.M. Carlucci, and T. Temesvari, J. Phys. I France **7**, 105 (1997).
 - ⁶¹ A. Crisanti and C. De Dominicis, Nucl. Phys. B **891**, 73 (2015).
 - ⁶² F. Antenucci, M. Ibañez Berganza, and L. Leuzzi, arXiv:1409.6345.
 - ⁶³ A. Marruzzo and L. Leuzzi, Phys. Rev. B **91**, 054201 (2015), arXiv:1411.4674.
 - ⁶⁴ A. Crisanti, H. Horner, and H.-J. Sommers, Z. Phys. B **92**, 257 (1993).
 - ⁶⁵ C. Weiss and R. Vilaseca, *Dynamics of lasers* (VCH, Weinheim (Germany), 1991).
 - ⁶⁶ A. Crisanti, M. Falcioni, and A. Vulpiani, Phys. Rev. Lett. **76**, 612 (1996).
 - ⁶⁷ R. Monasson, Phys. Rev. Lett. **75**, 2847 (1995).
 - ⁶⁸ M. Mézard, Physica A: Statistical Mechanics and its Applications **265**, 352 (1999).
 - ⁶⁹ M. Müller, L. Leuzzi, and A. Crisanti, Phys. Rev. B **74**, 134431 (2006).
 - ⁷⁰ A. Crisanti and L. Leuzzi, Phys. Rev. Lett. **93**, 217203 (2004).
 - ⁷¹ A. Crisanti and L. Leuzzi, Phys. Rev. B **75**, 144301 (2007).
 - ⁷² A. K. Tiwari and S. Mujumdar, Phys. Rev. Lett. **111**, 233903 (2013).
 - ⁷³ A. Crisanti and L. Leuzzi, Phys. Rev. B **73**, 014412 (2006).
 - ⁷⁴ F. Antenucci, M. Ibañez Berganza, and L. Leuzzi, (2015), arXiv:1412.8610.
 - ⁷⁵ C. De Dominicis and P. C. Martin, Journal of Mathematical Physics **5**, 14 (1964).
 - ⁷⁶ J. Cornwall, R. Jackiw, and E. Tomboulis, Physical Review D: Particles and Fields **10**, 2428 (1974).
 - ⁷⁷ R. Haymaker, Rivista del Nuovo Cimento **14**, 1 (1991).
 - ⁷⁸ T. Temesvari, C. D. Dominicis, and I. Kondor, J. Phys. A **27**, 7569 (1994).
 - ⁷⁹ Boundary terms from LA configurations contribute to $M_{u,v}^{r,r}$. These, however, are projected out by the Replica Fourier Transform and we can safely ignore them. For a more detailed discussion we refer to Ref. [61].
 - ⁸⁰ If $\overline{R} \leq 0$ the eigenvalue $1\Lambda(0; 1, 1)$ is replaced by $2\Lambda(0; 1, 1)$.
 - ⁸¹ T. H. Berlin and M. Kac, Phys. Rev. **86**, 821 (1952).